ATTACHMENT V

DOWNHOLE SEISMIC VELOCITY PLOTS (REDPATH) – WHB AREA

As discussed in Section 6.2.5, this attachment presents fifteen figures, one for each borehole surveyed by Redpath Geophysics, showing plots of adjusted travel time in milliseconds versus depth below ground surface in feet. The plots also show the linear fits to the data, the slope of which gives the velocity in feet per millisecond, which is converted to feet per second. Details of the surveys and data reduction can be found in scientific notebook SN-M&O-SCI-030-V1 (Wong 2002b).

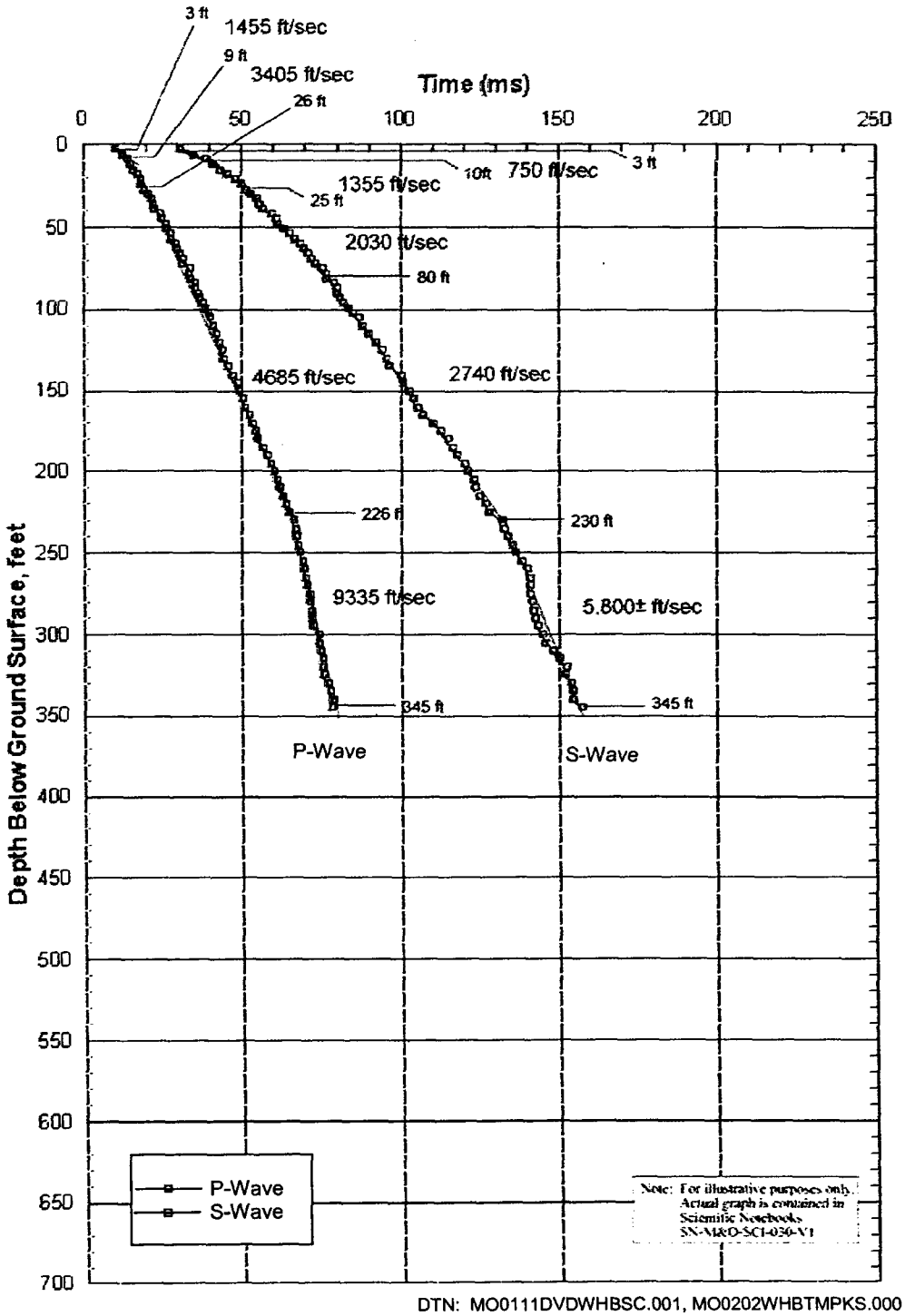

DTN: MO0111DVDWHBSC.001, MO0202WHBTMPKS.000

Figure V-1. RF#13 Downhole Travel Time Versus Depth

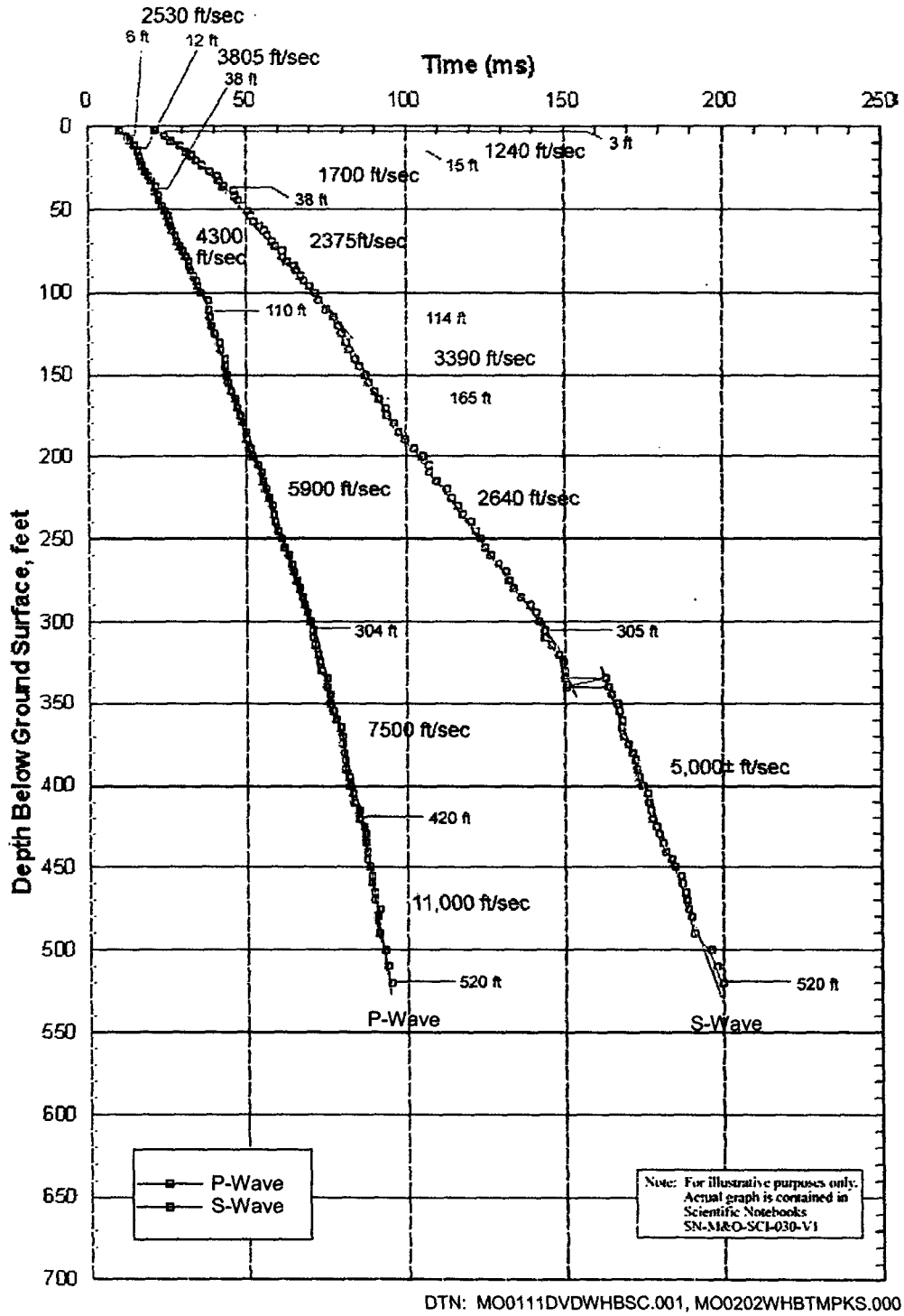

DTN: MO0111DVDWHBSC.001, MO0202WHBTMPKS.000

Figure V-2. RF#14 Downhole Travel Time Versus Depth

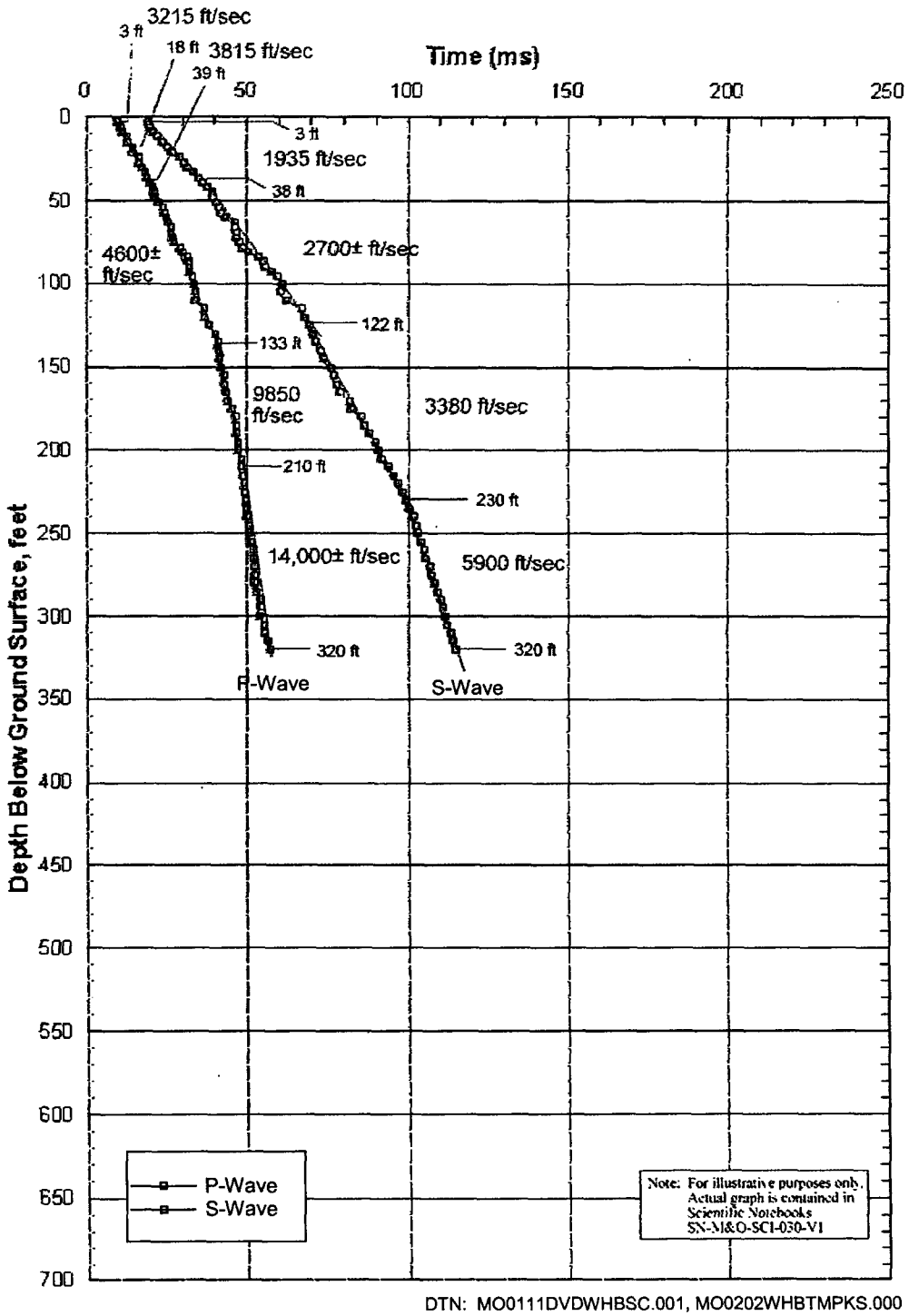

DTN: MO0111DVDWHBSC.001, MO0202WHBTMPKS.000

Figure V-3. RF#15 Downhole Travel Time Versus Depth

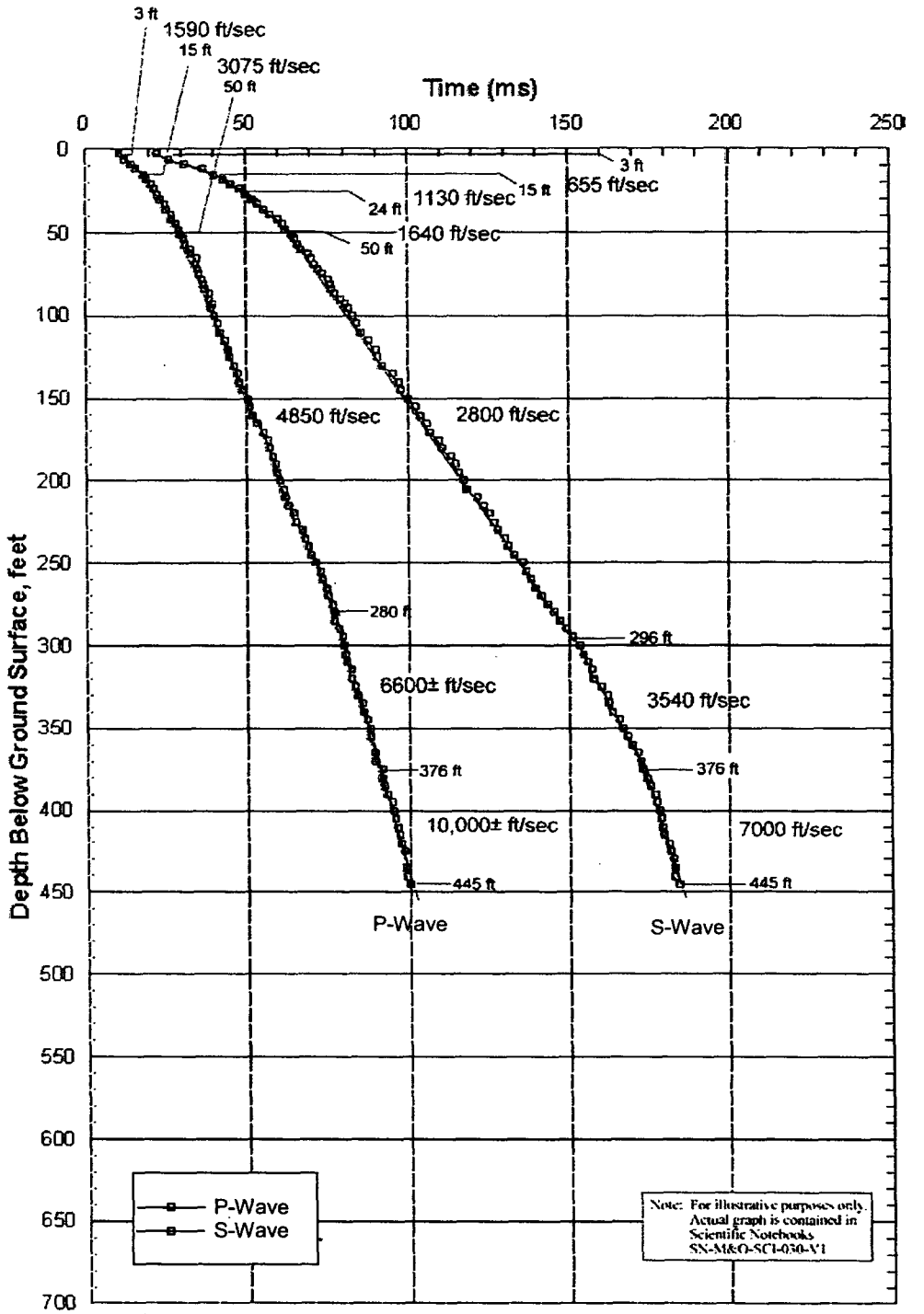

DTN: MO0111DVDWHBSC.001, MO0202WHBTMPKS.000

Figure V-4. RF#16 Downhole Travel Time Versus Depth

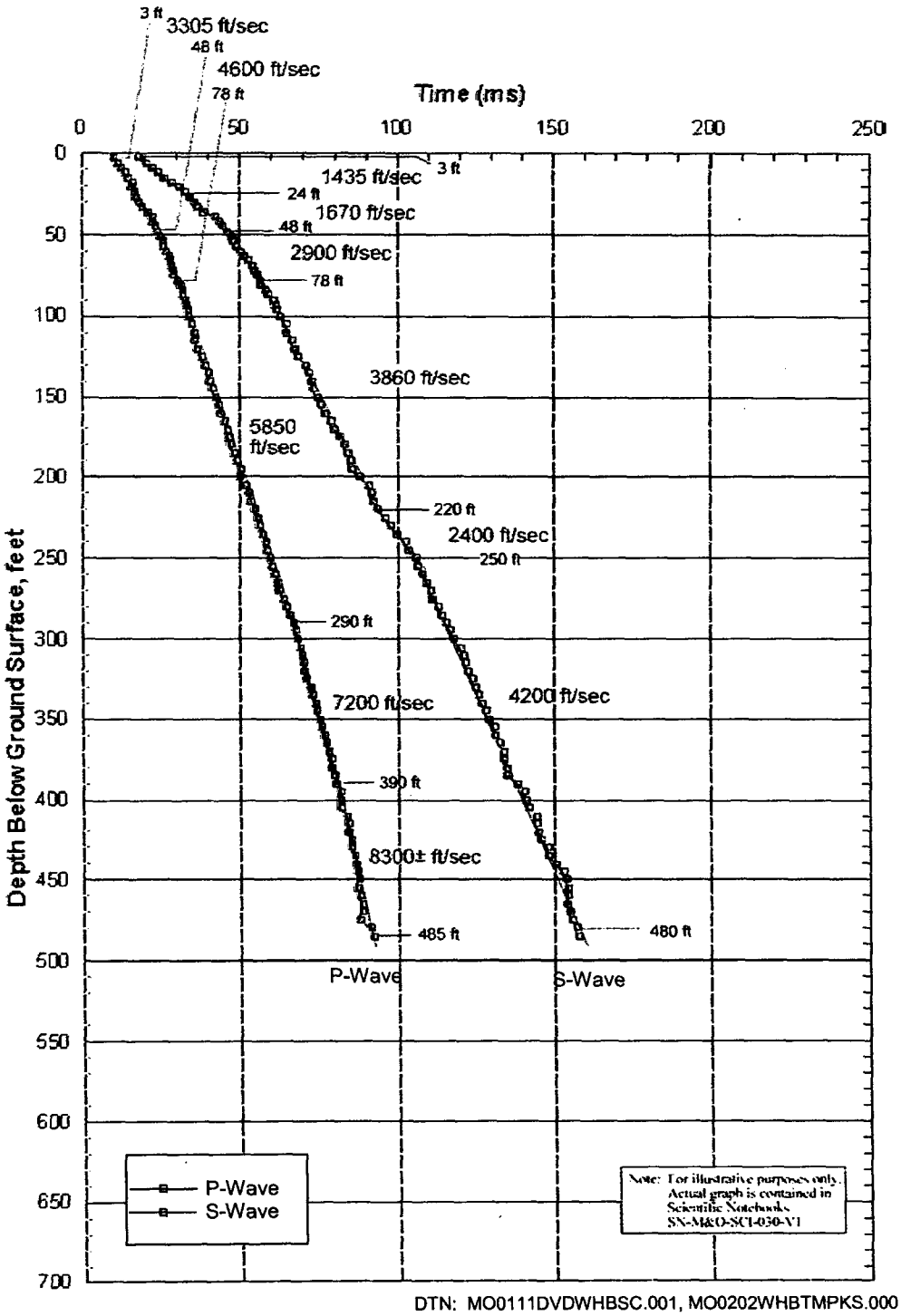

DTN: MO0111DVDWHBSC.001, MO0202WHBTMPKS.000

Figure V-5. RF#18 Downhole Travel Time Versus Depth

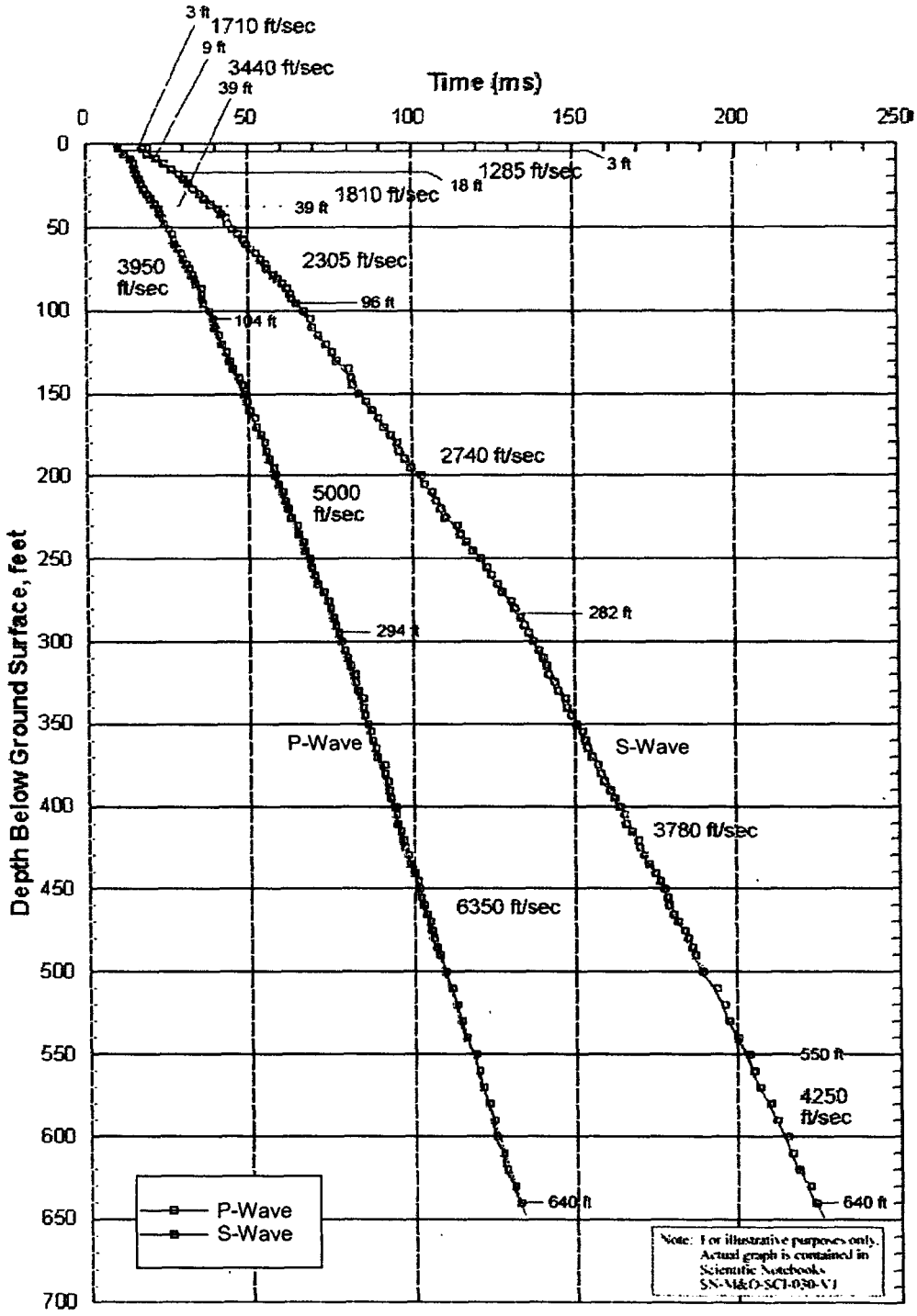

DTN: MO0111DVDWHBSC.001, MO0202WHBTMPKS.000

Figure V-6. RF#19 Downhole Travel Time Versus Depth

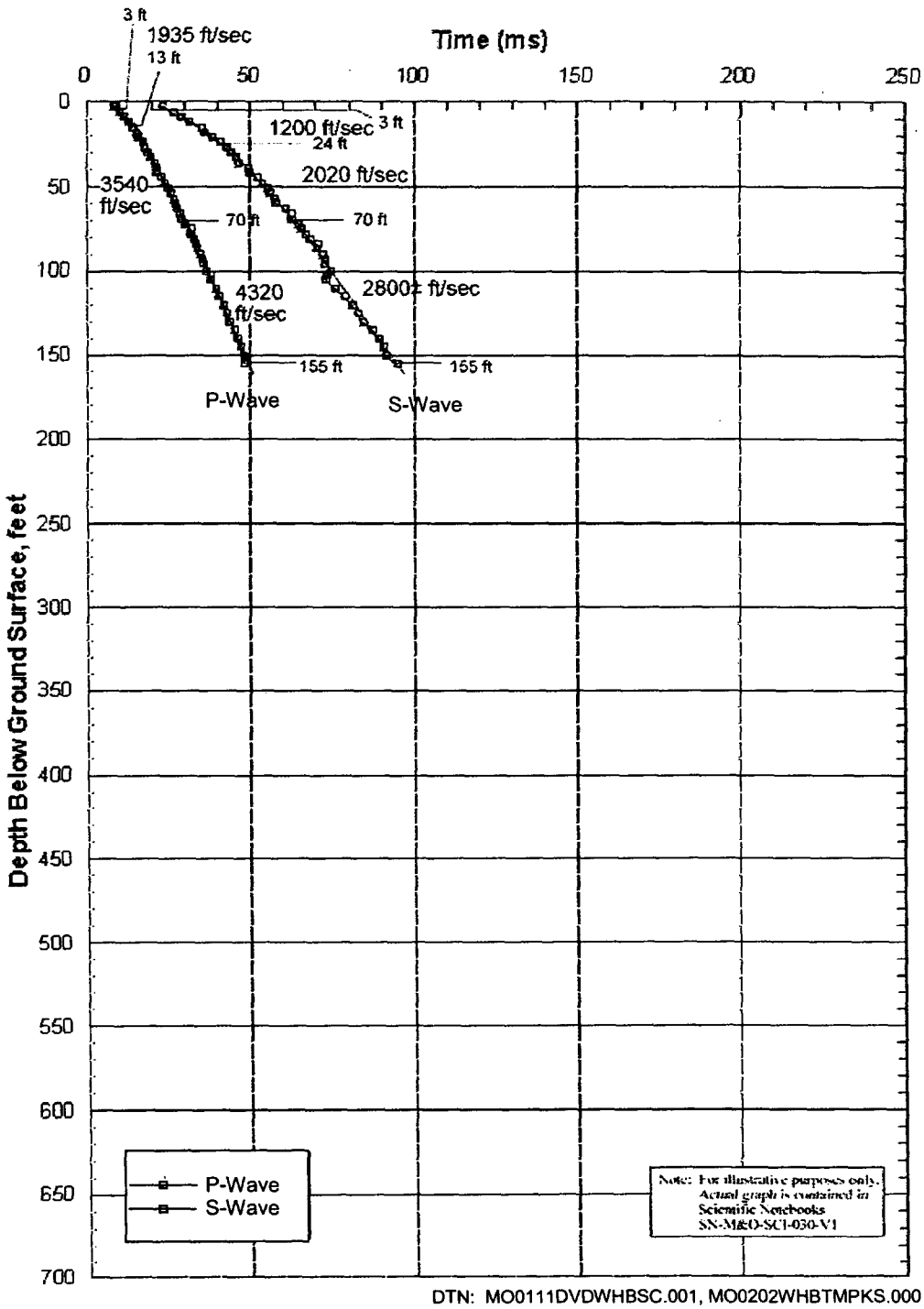

DTN: MO0111DVDWHBSC.001, MO0202WHBTMPKS.000

Figure V-7. RF#20 Downhole Travel Time Versus Depth

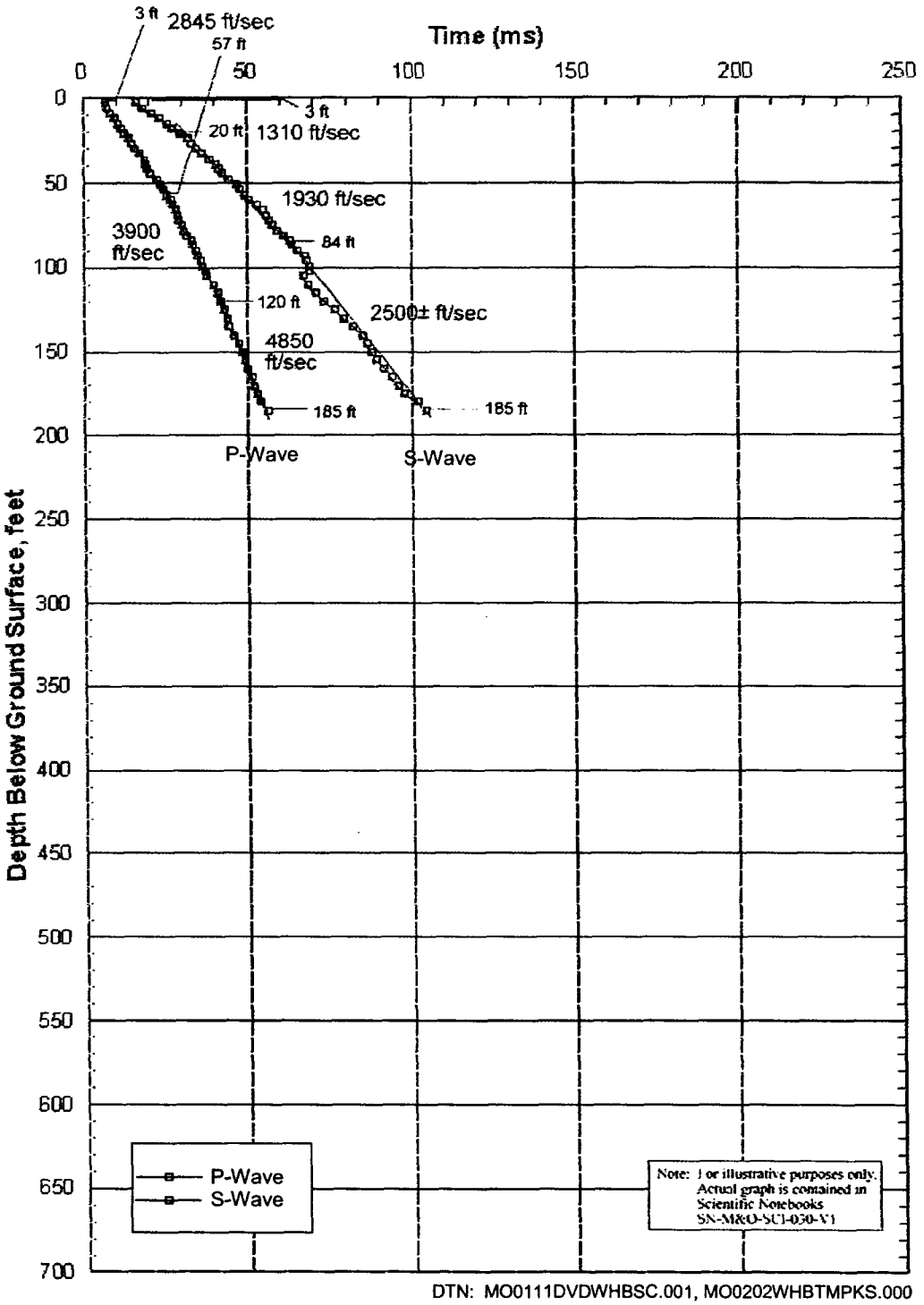

DTN: MO0111DVDWHBSC.001, MO0202WHBTMPKS.000

Figure V-8. RF#21 Downhole Travel Time Versus Depth

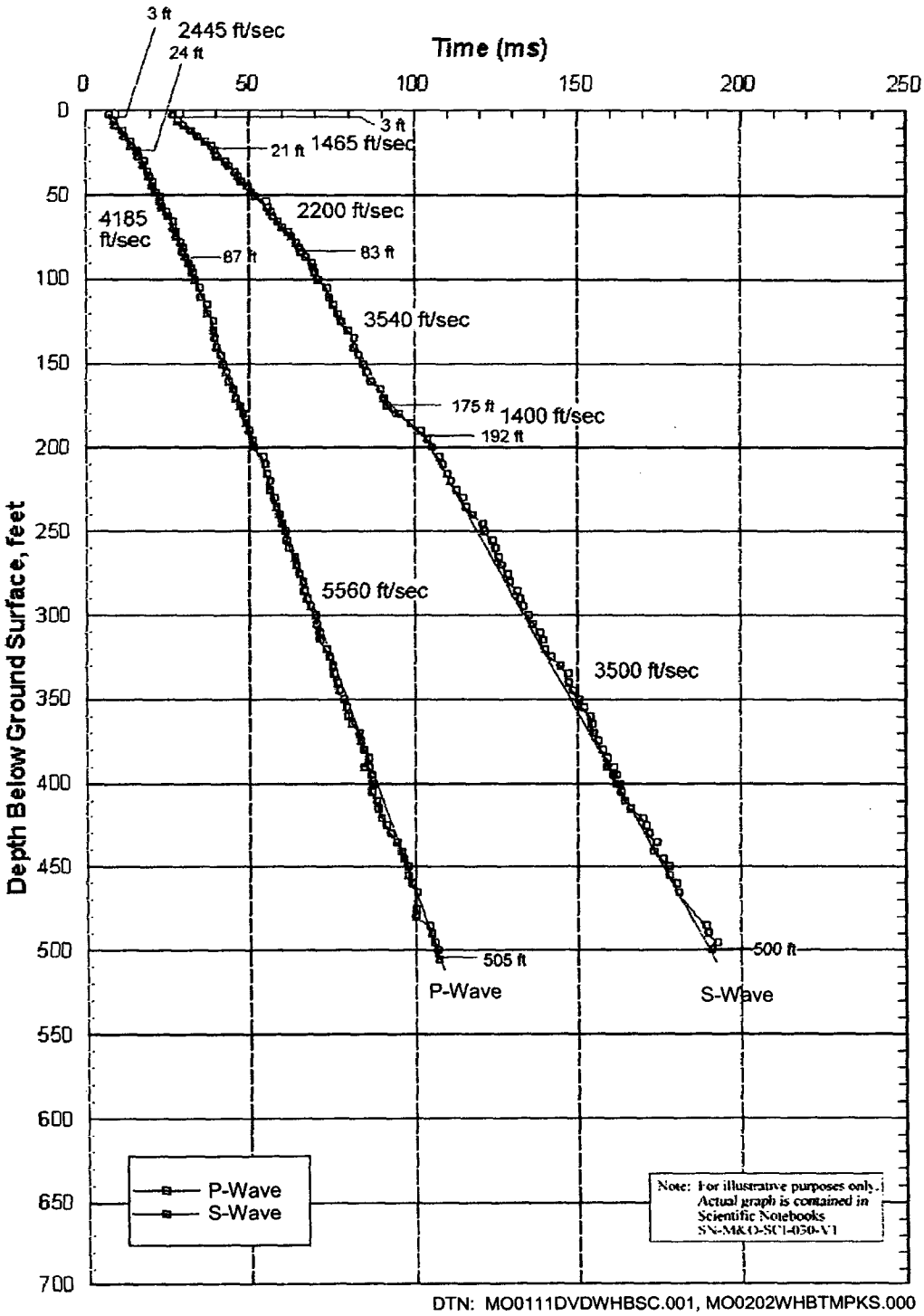

DTN: MO0111DVDWHBSC.001, MO0202WHBTMPKS.000

Figure V-9. RF#22 Downhole Travel Time Versus Depth

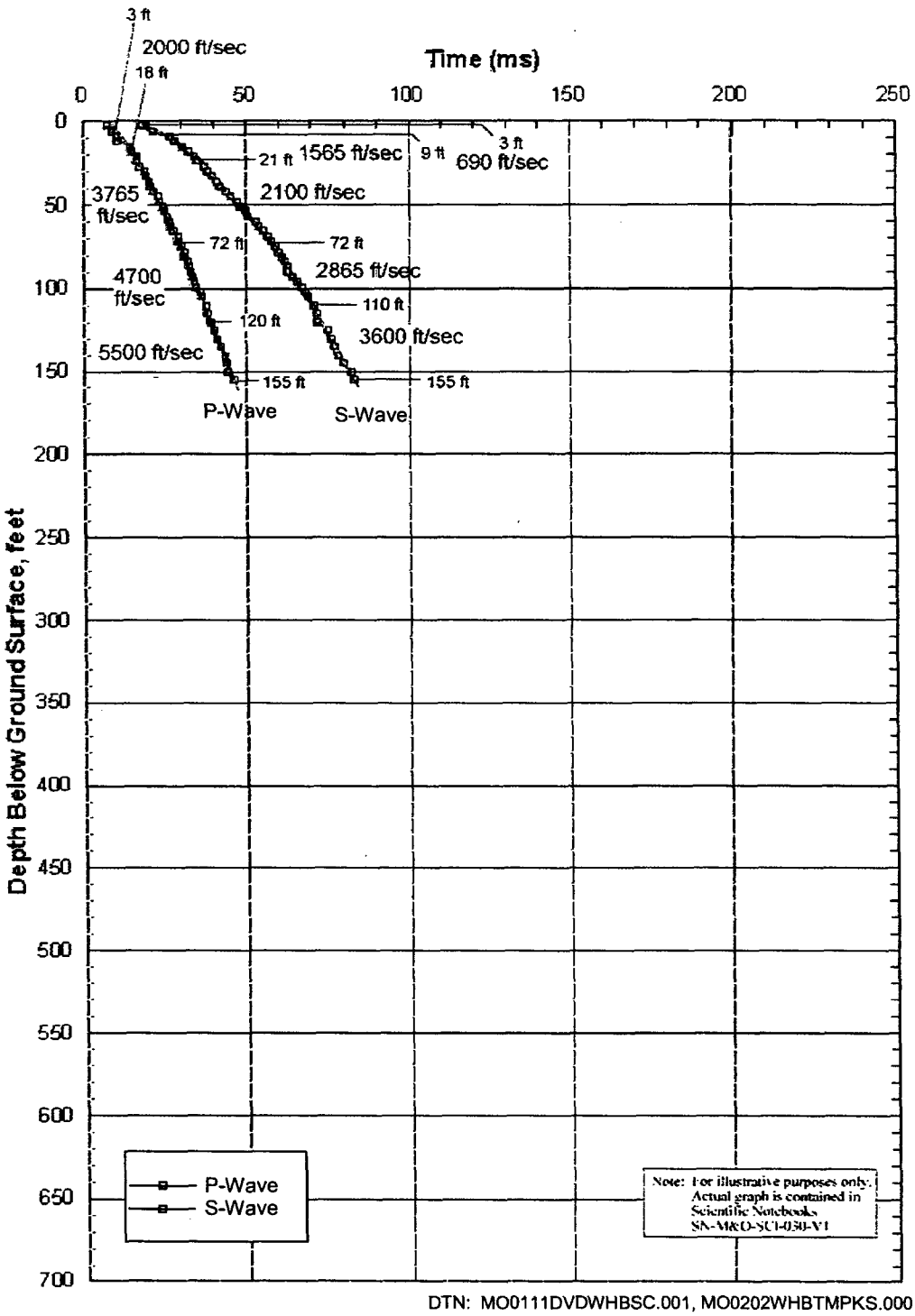

DTN: MO0111DVDWHBSC.001, MO0202WHBTMPKS.000

Figure V-10. RF#23 Downhole Travel Time Versus Depth

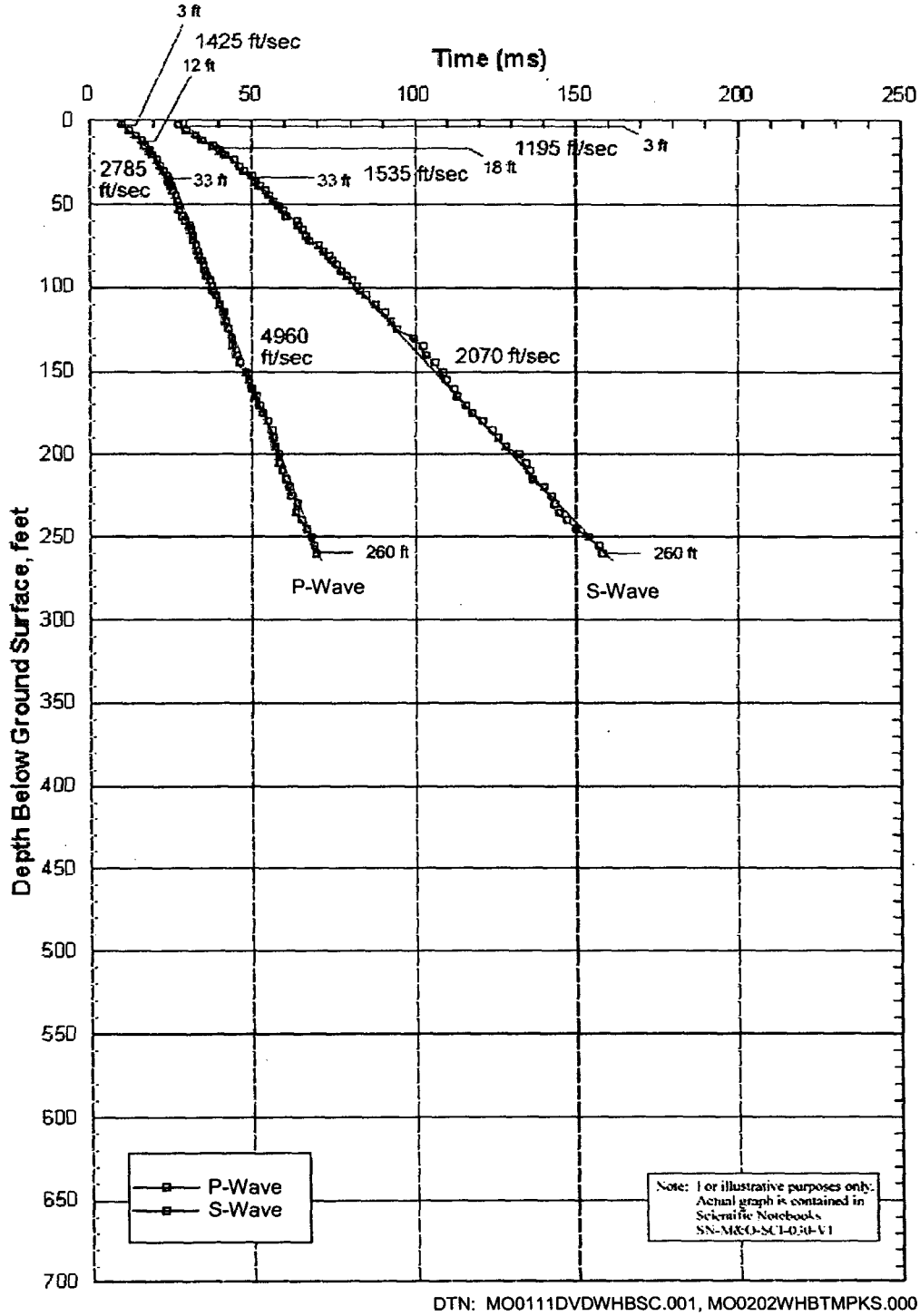

DTN: MO0111DVDWHBSC.001, MO0202WHBTMPKS.000

Figure V-11. RF#24 Downhole Travel Time Versus Depth

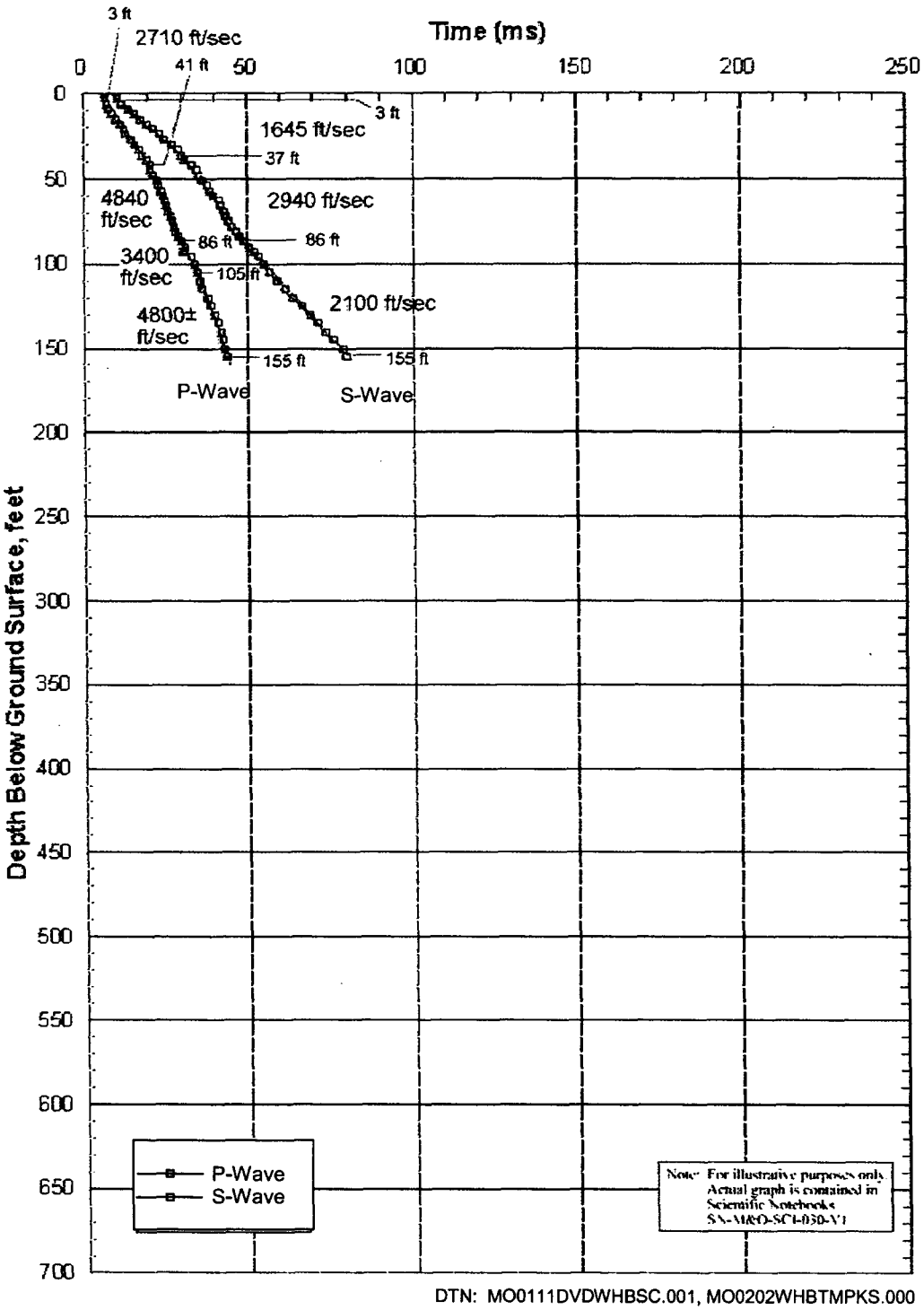

DTN: MO0111DVDWHBSC.001, MO0202WHBTMPKS.000

Figure V-12. RF#25 Downhole Travel Time Versus Depth

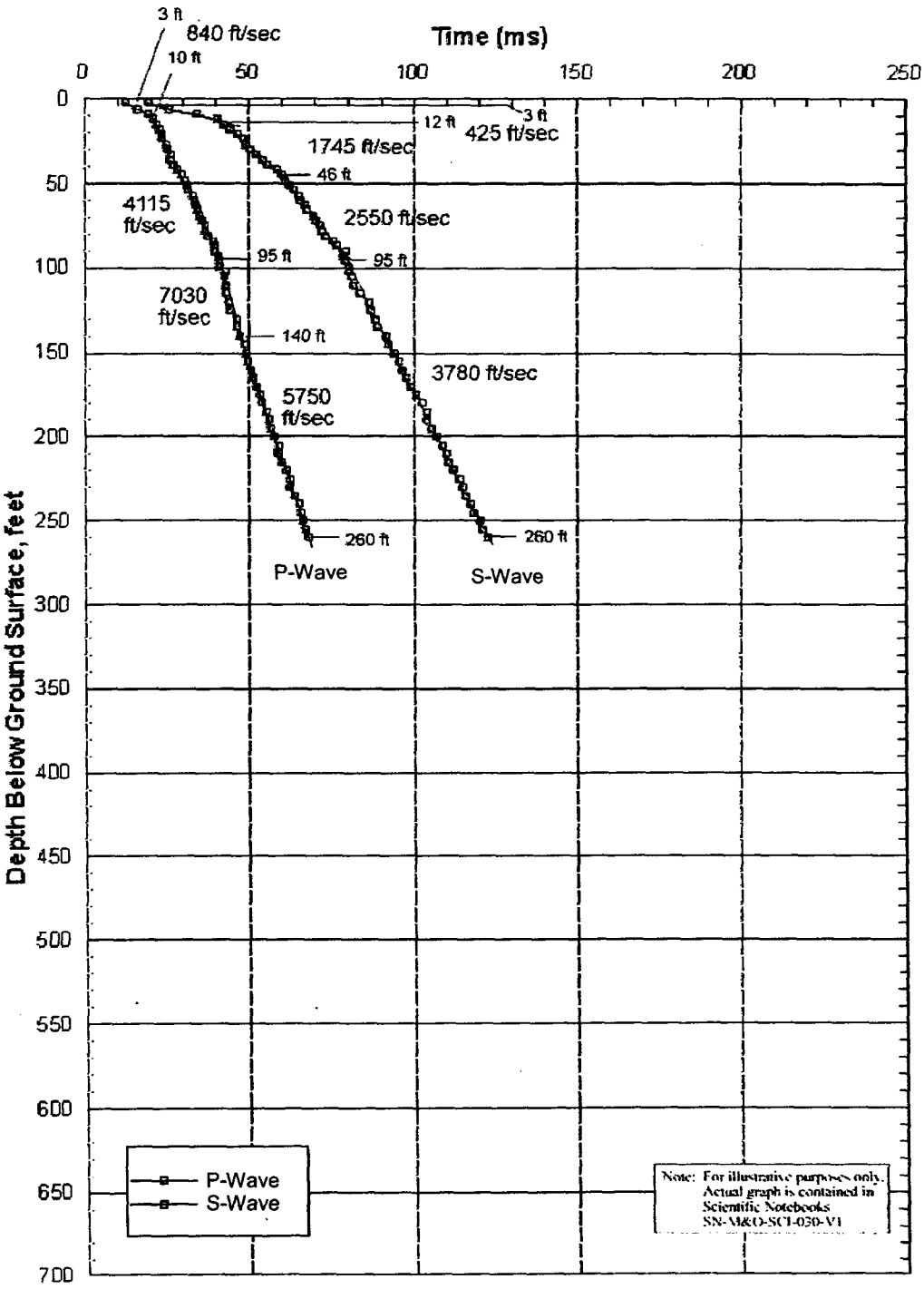

DTN: MO0111DVDWHBSC.001, MO0202WHBTMPKS.000

Figure V-13. RF#26 Downhole Travel Time Versus Depth

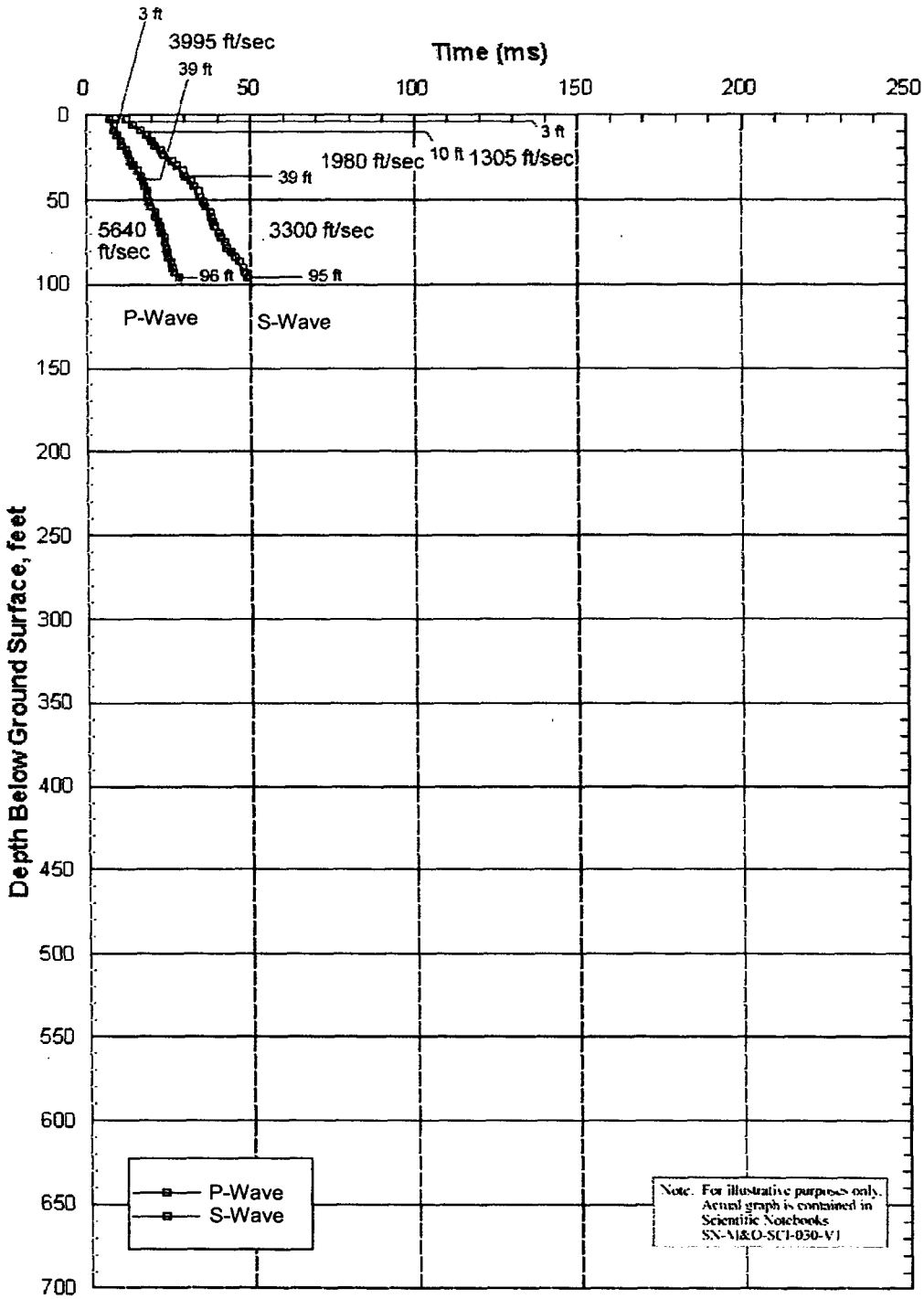

DTN: MO0111DVDWHBSC.001, MO0202WHBTMPKS.000

Figure V-14. RF#28 Downhole Travel Time Versus Depth

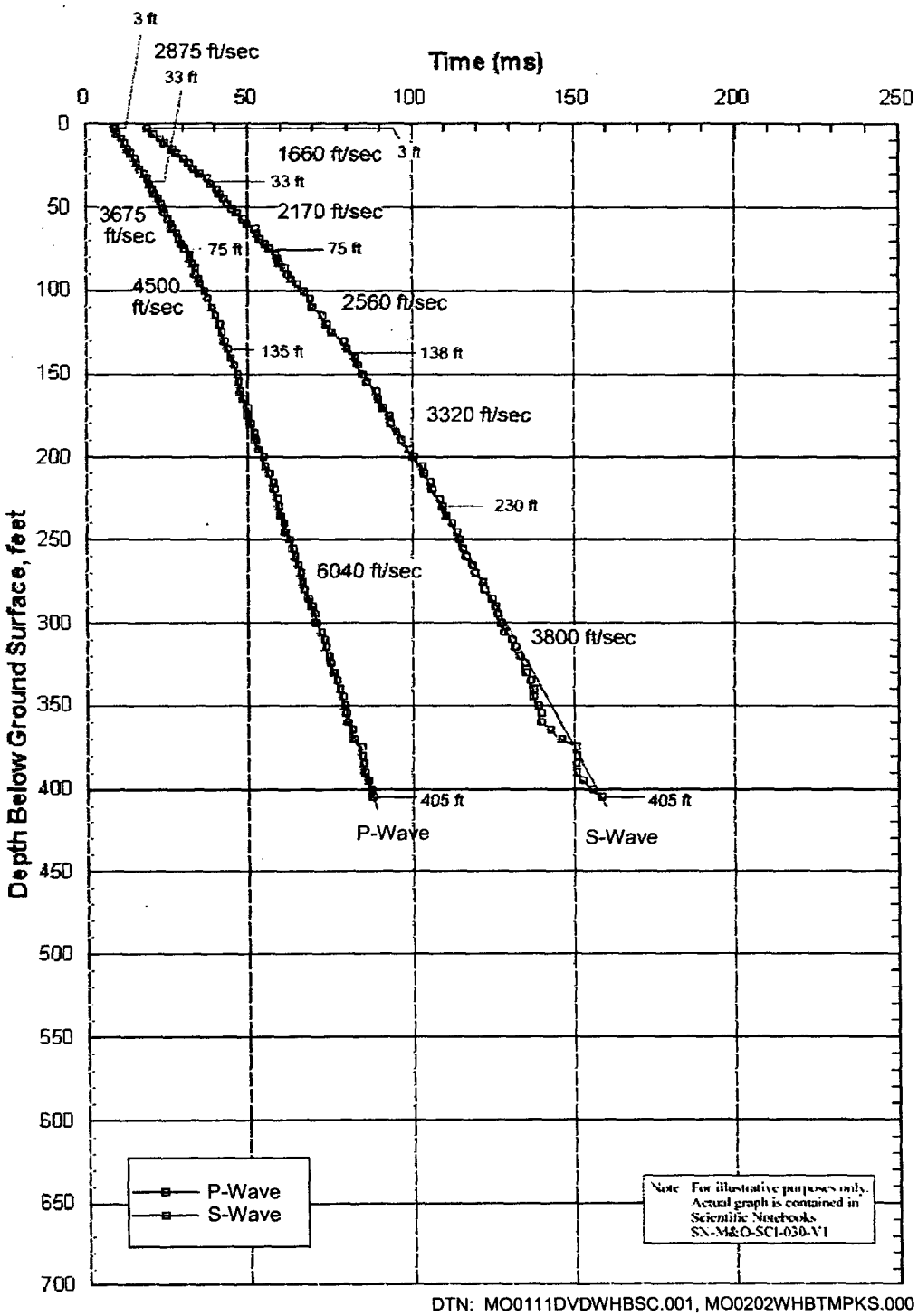

DTN: MO0111DVDWHBSC.001, MO0202WHBTMPKS.000

Figure V-15. RF#29 Downhole Travel Time Versus Depth

ATTACHMENT VI

DOWNHOLE SEISMIC VELOCITY PLOTS (GEOVISION) – WHB AREA

ATTACHMENT VI

DOWNHOLE SEISMIC VELOCITY PLOTS (GEOVISION) – WHB AREA

As discussed in Section 6.2.5, this attachment presents four figures, two for each of boreholes RF#13 and #17 surveyed by GEOVision, Inc., showing plots of adjusted travel time in milliseconds versus depth below ground surface in feet. The plots also show the linear fits to the data, the slope of which gives the velocity in feet per millisecond, which is converted to feet per second. One interpretation was made by picking the first break (initial arrival) of the shear or compression wave for records at all depths, and a second interpretation was made by picking the peak of the first appearance of the shear or compression wave. GEOVision prefers the first break approach, but also provided the first peak interpretation for comparison purposes. Comparisons of Figures VI-1 and VI-2 and of Figures VI-3 and VI-4 show that the two interpretations agree very well. Details of the surveys and data reduction can be found in scientific notebook SN-M&O-SCI-025-V1 (Luebbers 2002c).

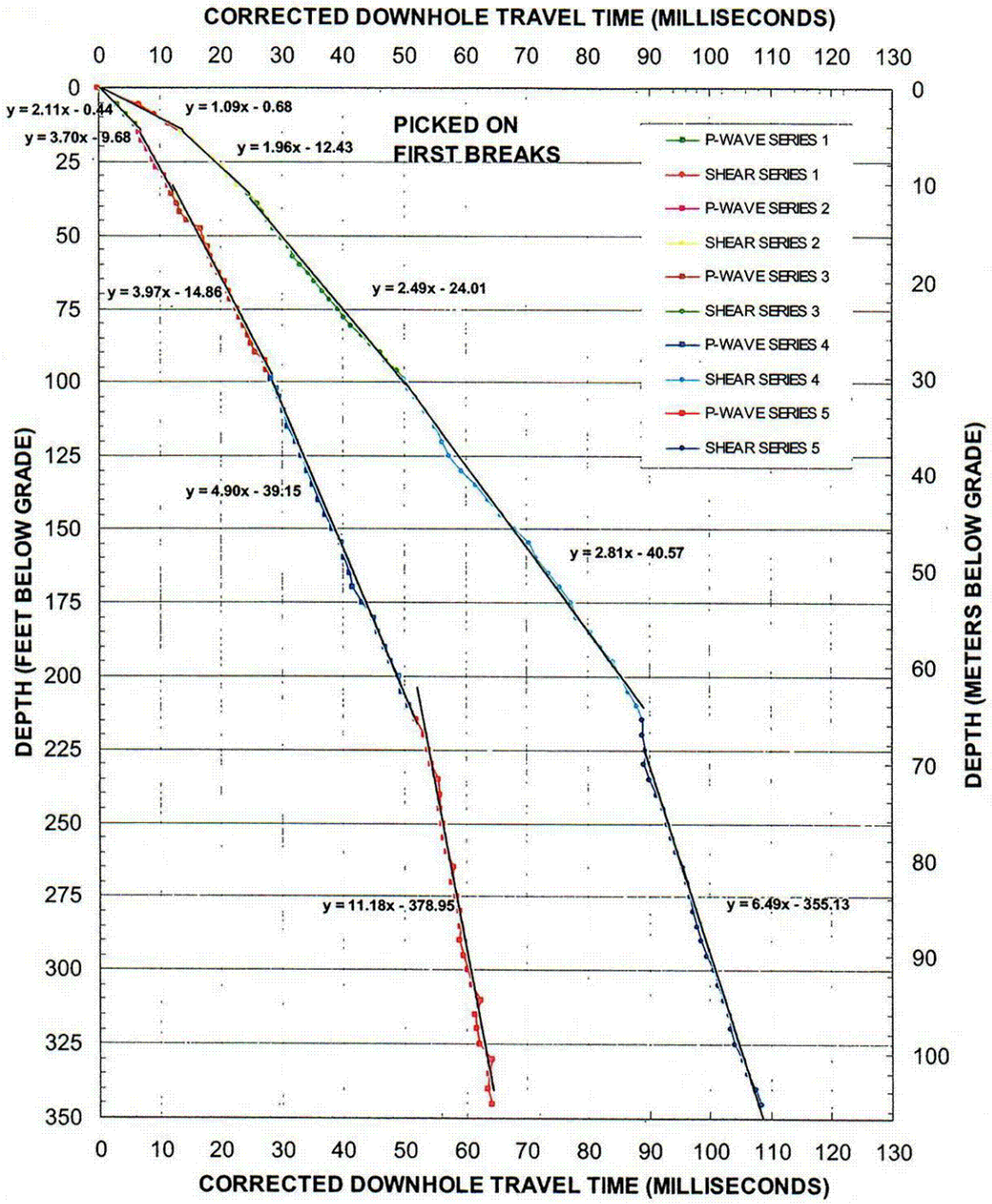

DTN: MO0110DVDBOREH.000, MO0202DWAVEATD.000

Figure VI-1. RF#13 Downhole Travel Time Versus Depth Plots (First Break Picks)

C01

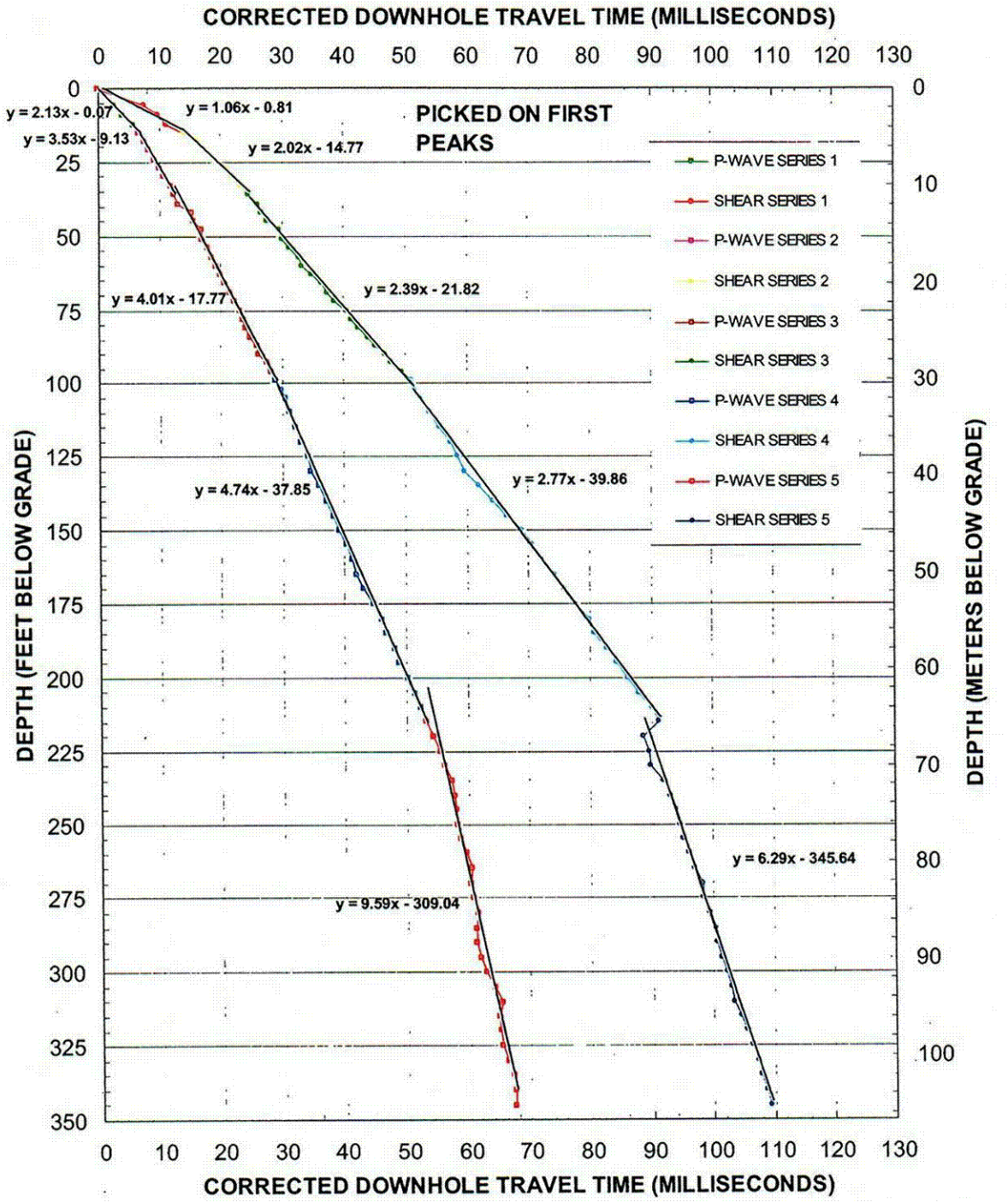

DTN: MO0110DVDBOREH.000, MO0202DWAVEATD.000

Figure VI-2. RF#13 Downhole Travel Time Versus Depth Plots (Peak Picks)

C02

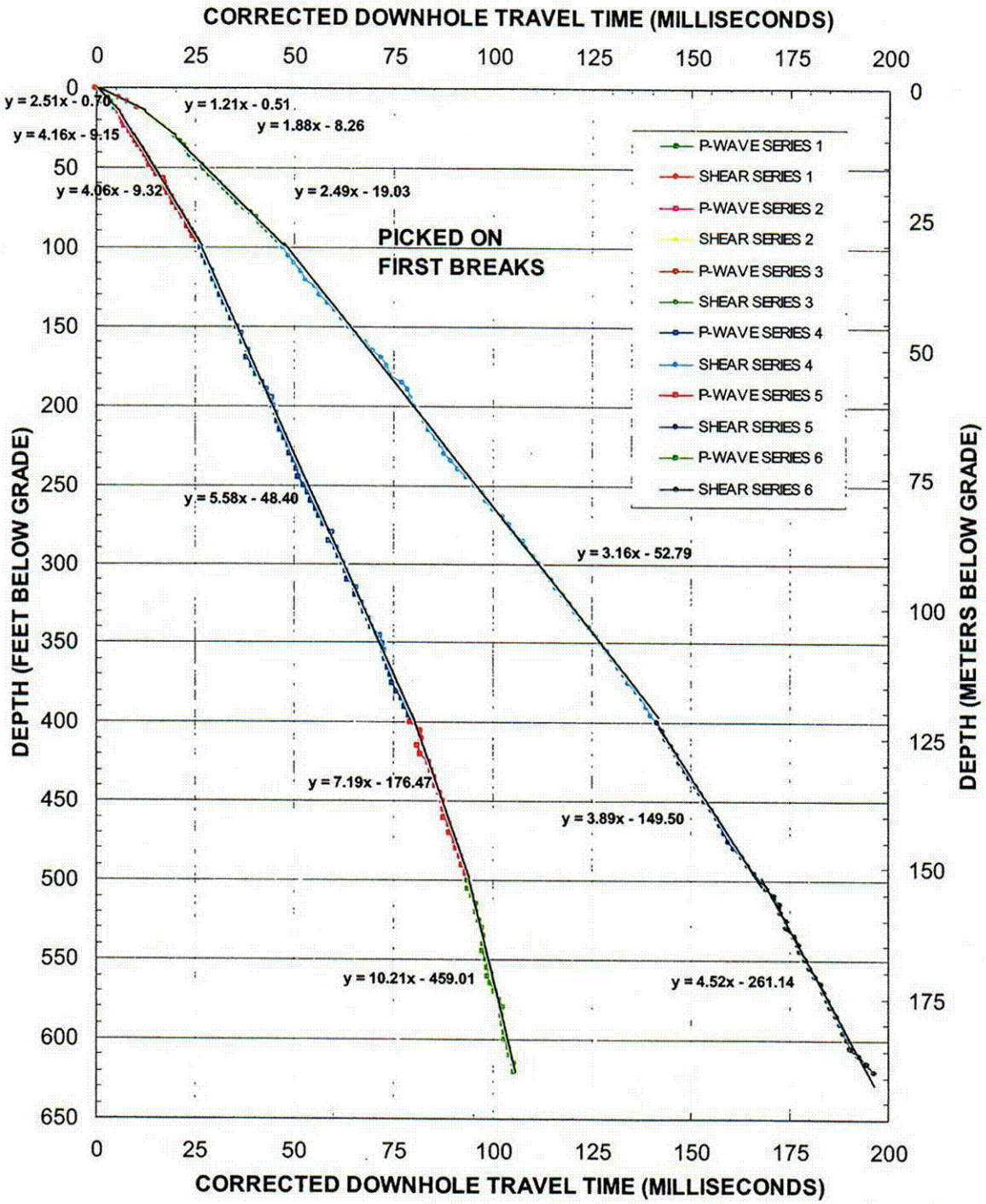

DTN: MO0110DVDBOREH.000, MO0202DWAVEATD.000

Figure VI-3. RF#17 Downhole Travel Time Versus Depth Plots (First Break Picks)

C03

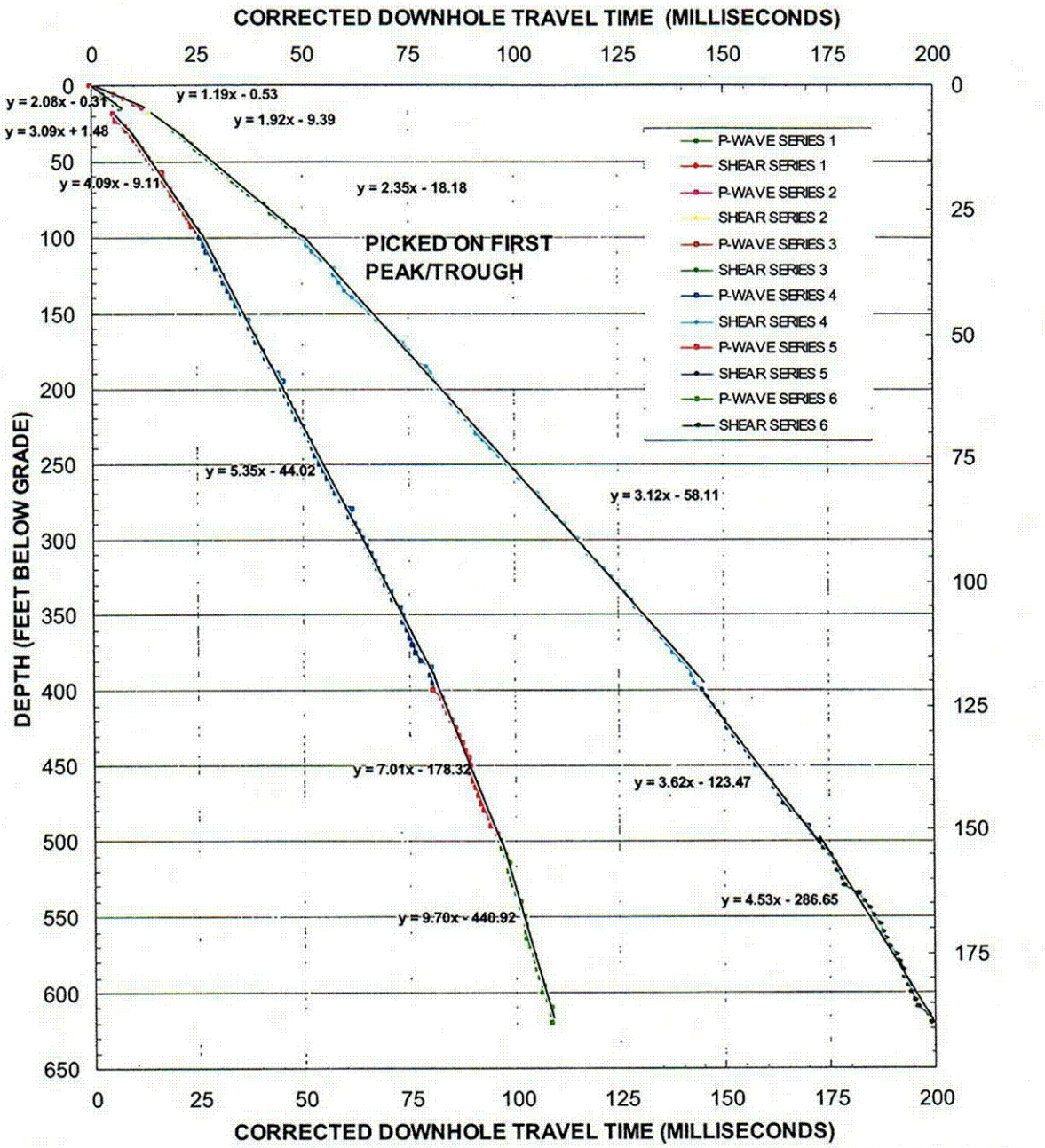

DTN: MO0110DVDBOREH.000, MO0202DWAVEATD.000

Figure VI-4. RF#17 Downhole Travel Time Versus Depth Plots (Peak Picks)

C04

ATTACHMENT VII

SUSPENSION SEISMIC INTERVAL VELOCITY PLOTS

ATTACHMENT VII

SUSPENSION SEISMIC INTERVAL VELOCITY PLOTS

As mentioned in Section 6.2.6.4, this attachment presents plots and tables of interpreted suspension seismic measurements as follows:

- Figures VII-1 through VII-16, plots of shear-wave interval velocity vs. depth bgs at boreholes RF#13 through RF#29, respectively.
- Figures VII-17 through VII-32, plots of compression-wave interval velocity vs. depth bgs at boreholes RF#13 through RF#29, respectively.
- Figures VII-33 through VII-48, plots of Poisson's ratio derived from interval velocity measurements vs. depth bgs at boreholes RF#13 through RF#29, respectively.
- Figures VII-49 and VII-50 plot the averaged shear-wave velocity for individual boreholes together with the median and median ± one standard deviation for the entire data set.
- Figure VII-51 plots the averaged compression-wave velocity for individual boreholes together with the median and median ± one standard deviation for the entire data set.
- Figure VII-52 plots the values of Poisson's ratio calculated from the averaged shear- and compression-wave velocity for individual boreholes together with the median and median ± one standard deviation for the entire data set.
- Tables VII-1 and VII-2 present values of mean, median, standard deviation, and coefficient of variation and count (number of measurements in the data set) by lithostratigraphic unit for receiver-to-receiver and source-to-receiver measurements, respectively.
- Table VII-3 summarizes mean, median, standard deviation, and coefficient of variation and count by lithostratigraphic unit for the compression-wave velocity values.
- Table VII-4 summarizes mean, median, standard deviation, and coefficient of variation and count by lithostratigraphic unit for the Poisson's ratio values.

As a reminder, the 2000-1 downhole seismic survey was performed by Redpath Geophysics and the 2000-1 downhole seismic survey was performed by GEOVision.

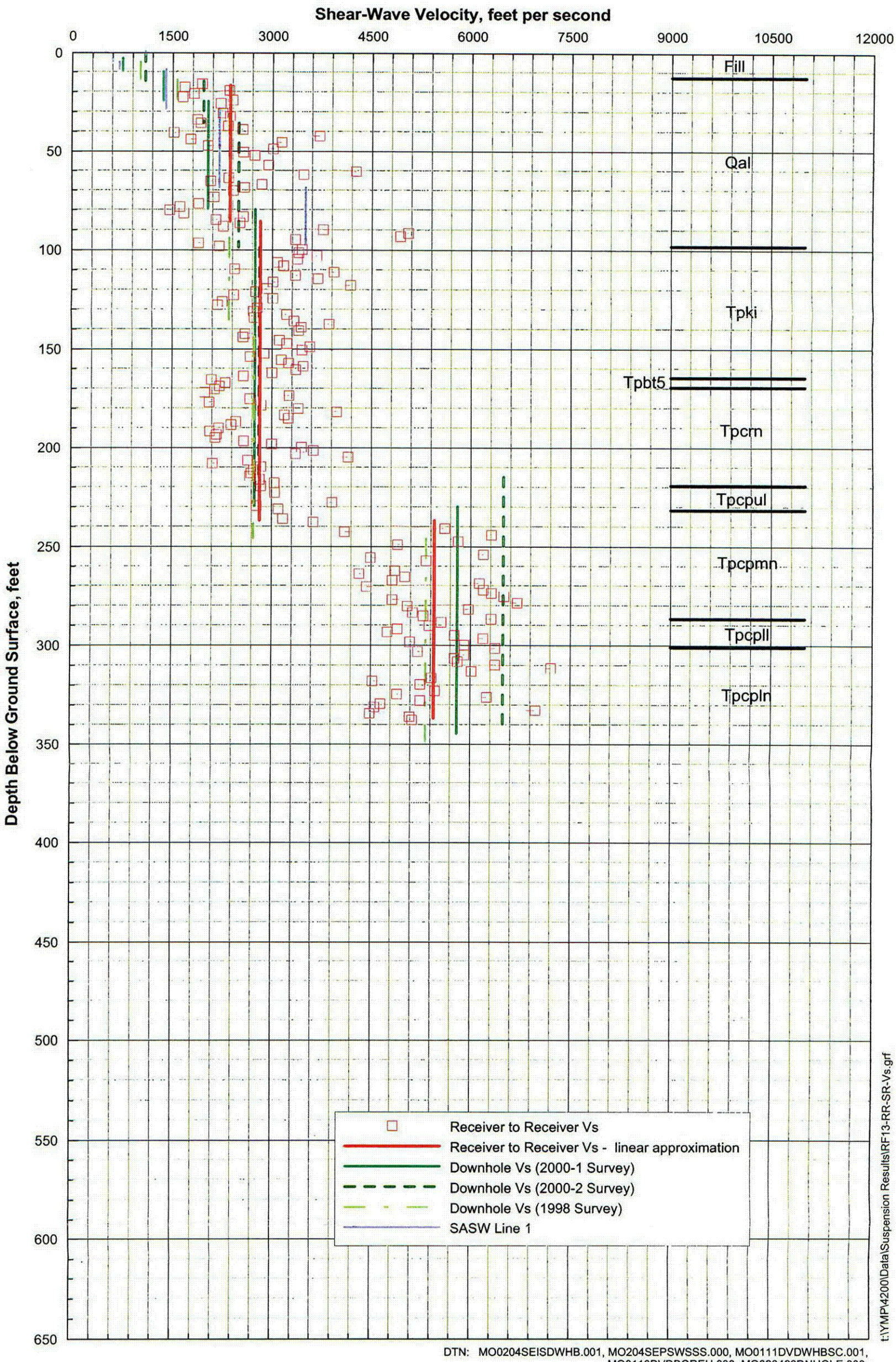

DTN: MO0204SEISDWHB.001, MO204SEPSWSSS.000, MO0111DVDWHBSC.001, MO0110DVDBOREH.000, MO020498DNHOLE.000, MO0110SASWWHBS.000, GS020383114233.003

NOTE: Downhole and SASW velocities are shown for comparison.

Figure VII-1. Shear-Wave Velocity (v_S) from Suspension Seismic Receiver-to-Receiver Data at Borehole RF#13.

C05

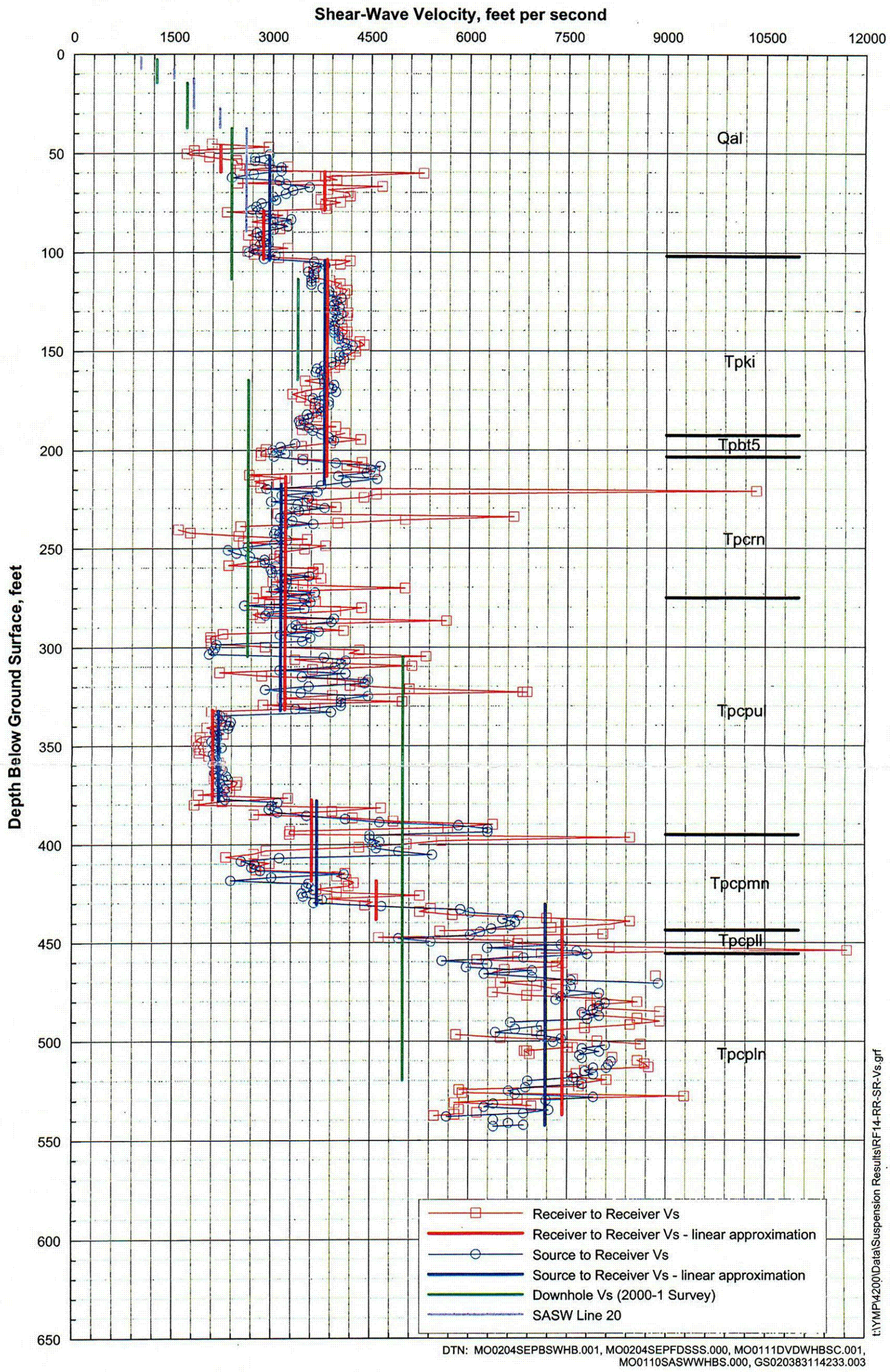

NOTE: Downhole and SASW velocities are shown for comparison.

Figure VII-2. Shear-Wave Velocity (v_S) from Suspension Seismic Source-to-Receiver and Receiver-to-Receiver Data at Borehole RF#14.

C06

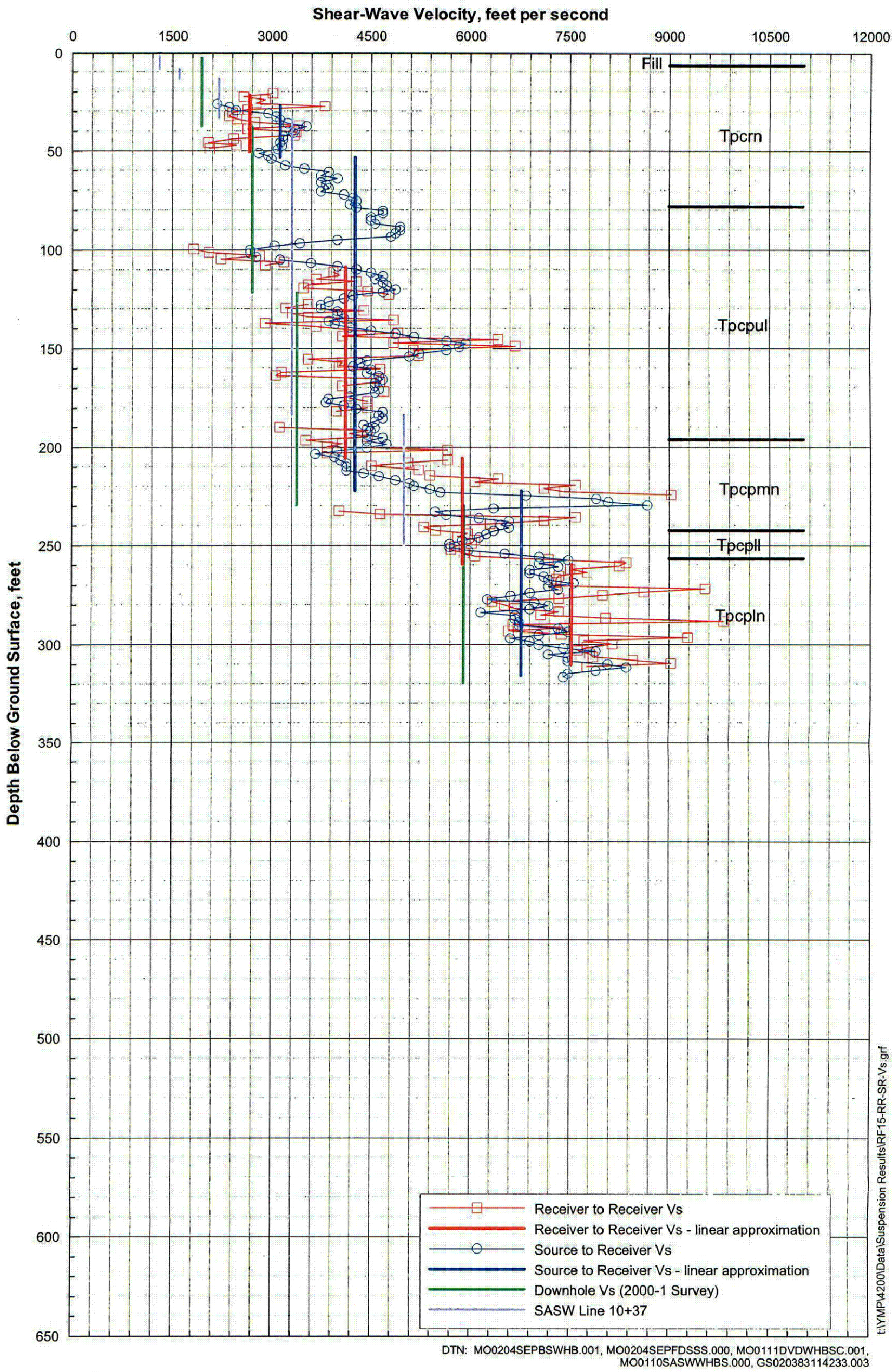

NOTE: Downhole and SASW velocities are shown for comparison.

Figure VII-3. Shear-Wave Velocity (v_S) from Suspension Seismic Source-to-Receiver and Receiver-to-Receiver Data at Borehole RF#15.

C07

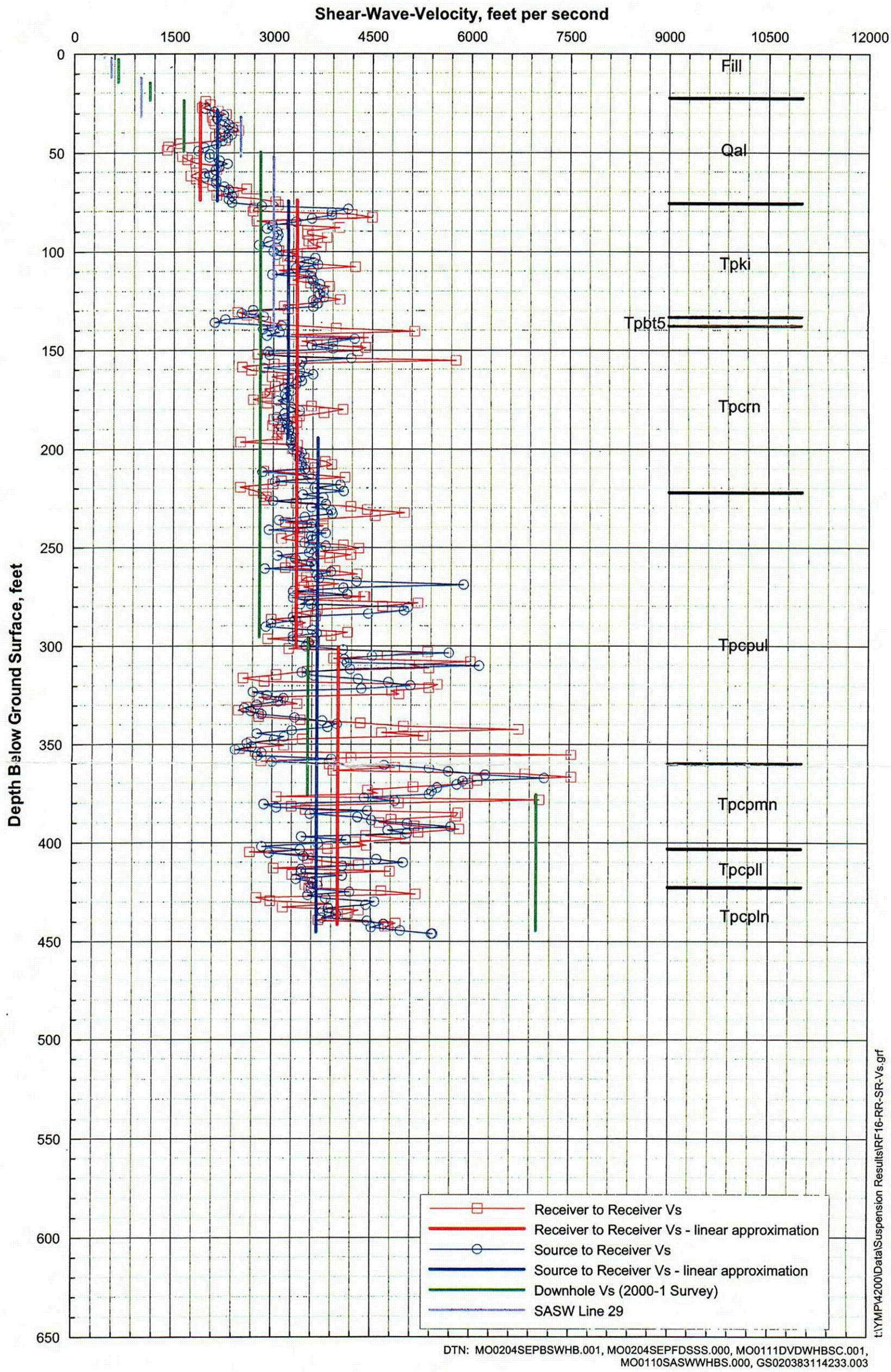

DTN: MO0204SEPBSWHB.001, MO0204SEPFDSSS.000, MO0111DVDWHBSC.001, MO0110SASWWHBS.000, GS020383114233.003

NOTE: Downhole and SASW velocities are shown for comparison.

Figure VII-4. Shear Wave Velocity (v_S) from Suspension Seismic Source-to-Receiver and Receiver-to-Receiver Data at Borehole RF#16.

C08

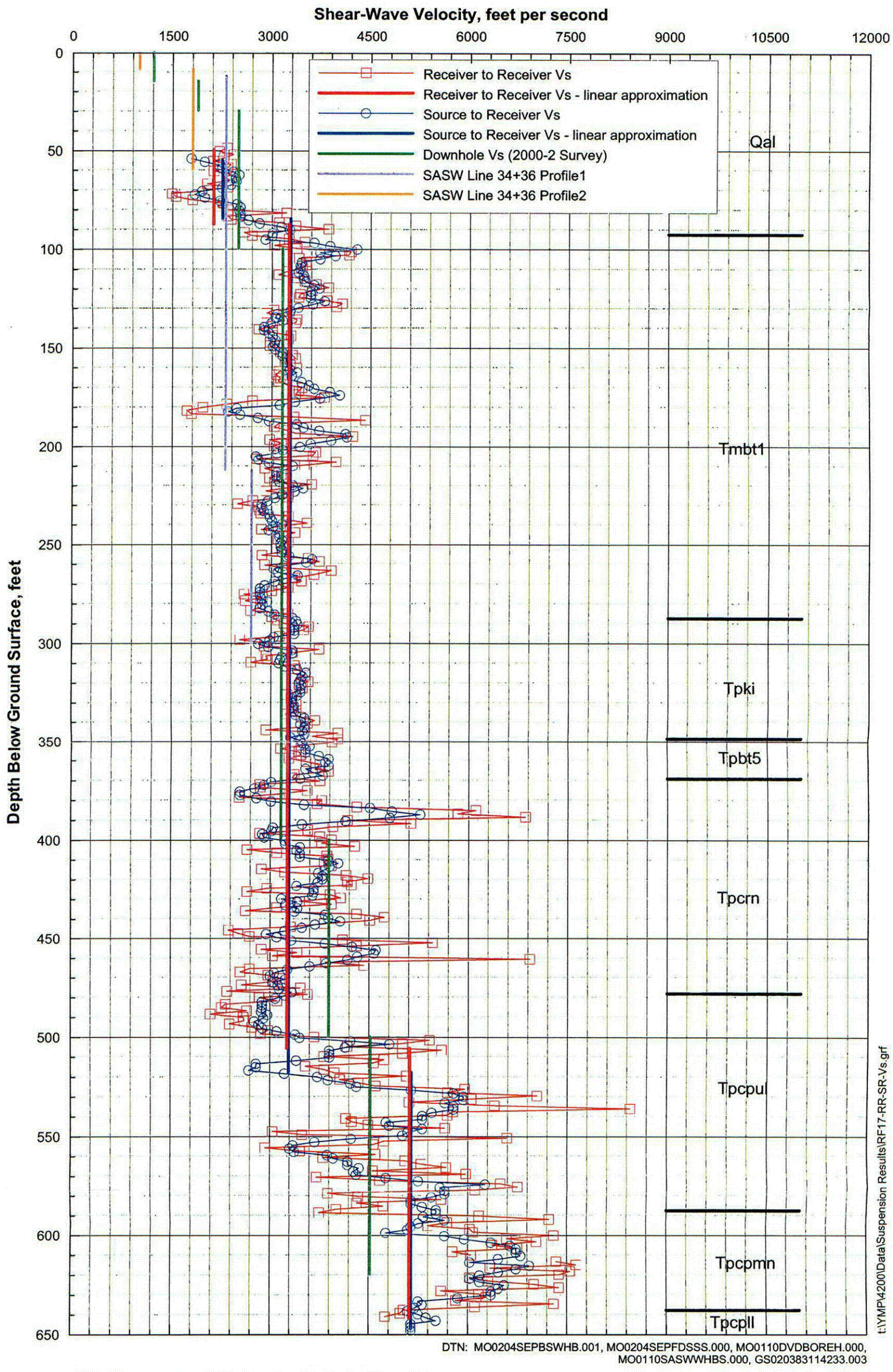

NOTE: Downhole and SASW velocities are shown for comparison.

Figure VII-5. Shear-Wave Velocity (v_S) from Suspension Seismic Source-to-Receiver and Receiver-to-Receiver Data at Borehole RF#17.

C09

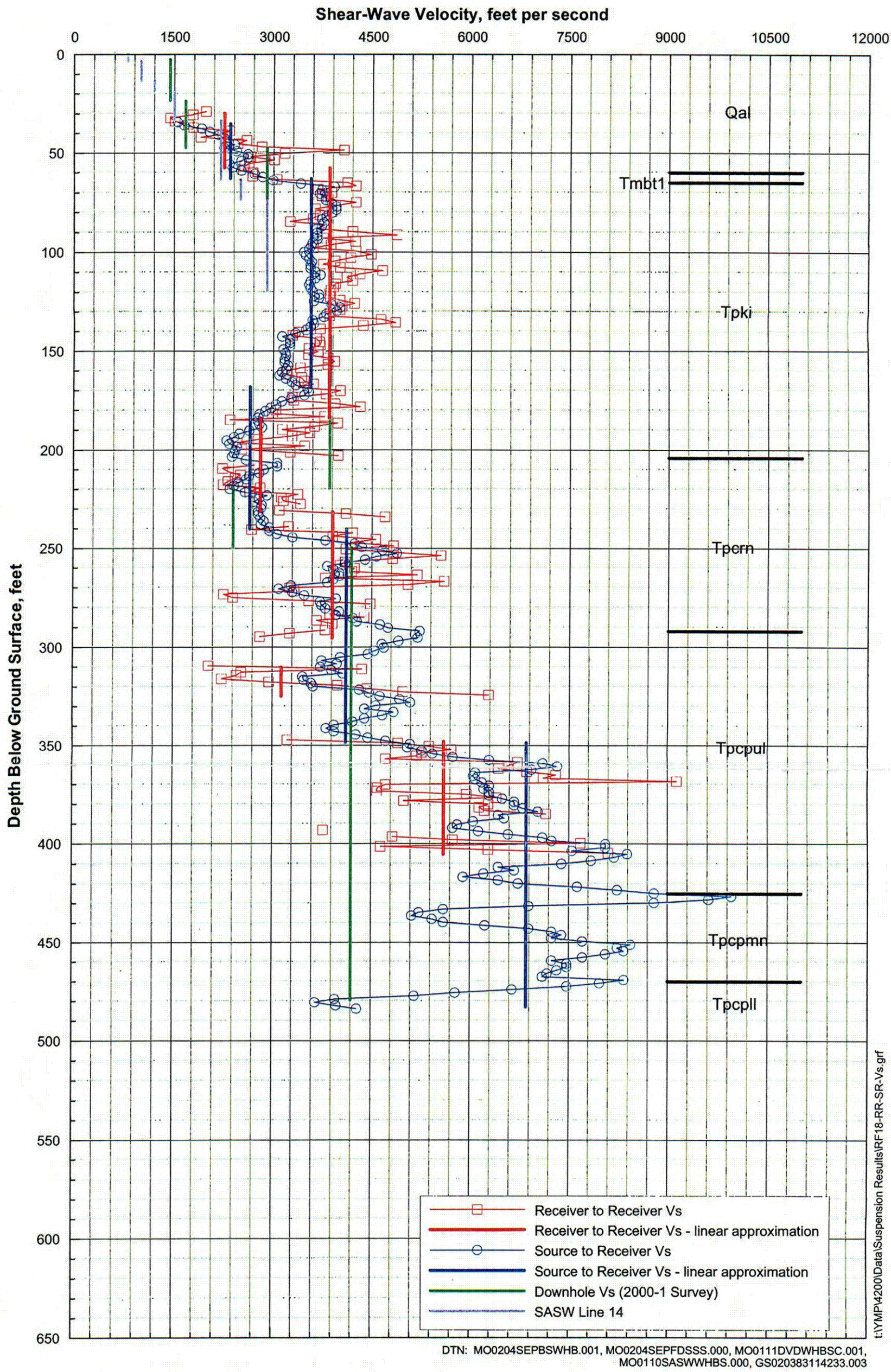

NOTE: Downhole and SASW velocities are shown for comparison.

Figure VII-6. Shear-Wave Velocity (v_S) from Suspension Seismic Source-to-Receiver and Receiver-to-Receiver Data at Borehole RF#18.

C10

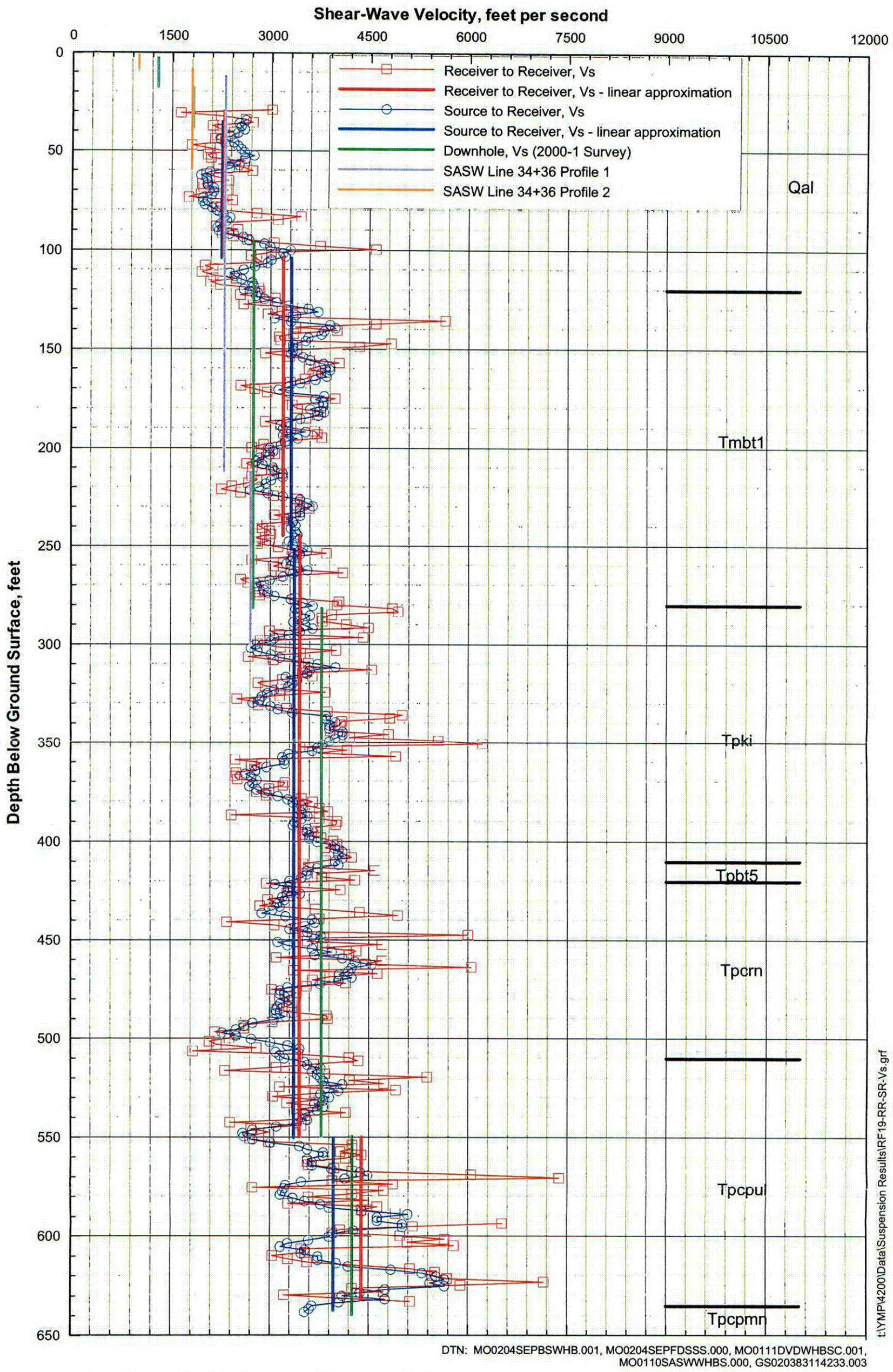

NOTE: Downhole and SASW velocities are shown for comparison.

Figure VII-7. Shear-Wave Velocity (v_S) from Suspension Seismic Source-to-Receiver and Receiver-to-Receiver Data at Borehole RF#19.

C11

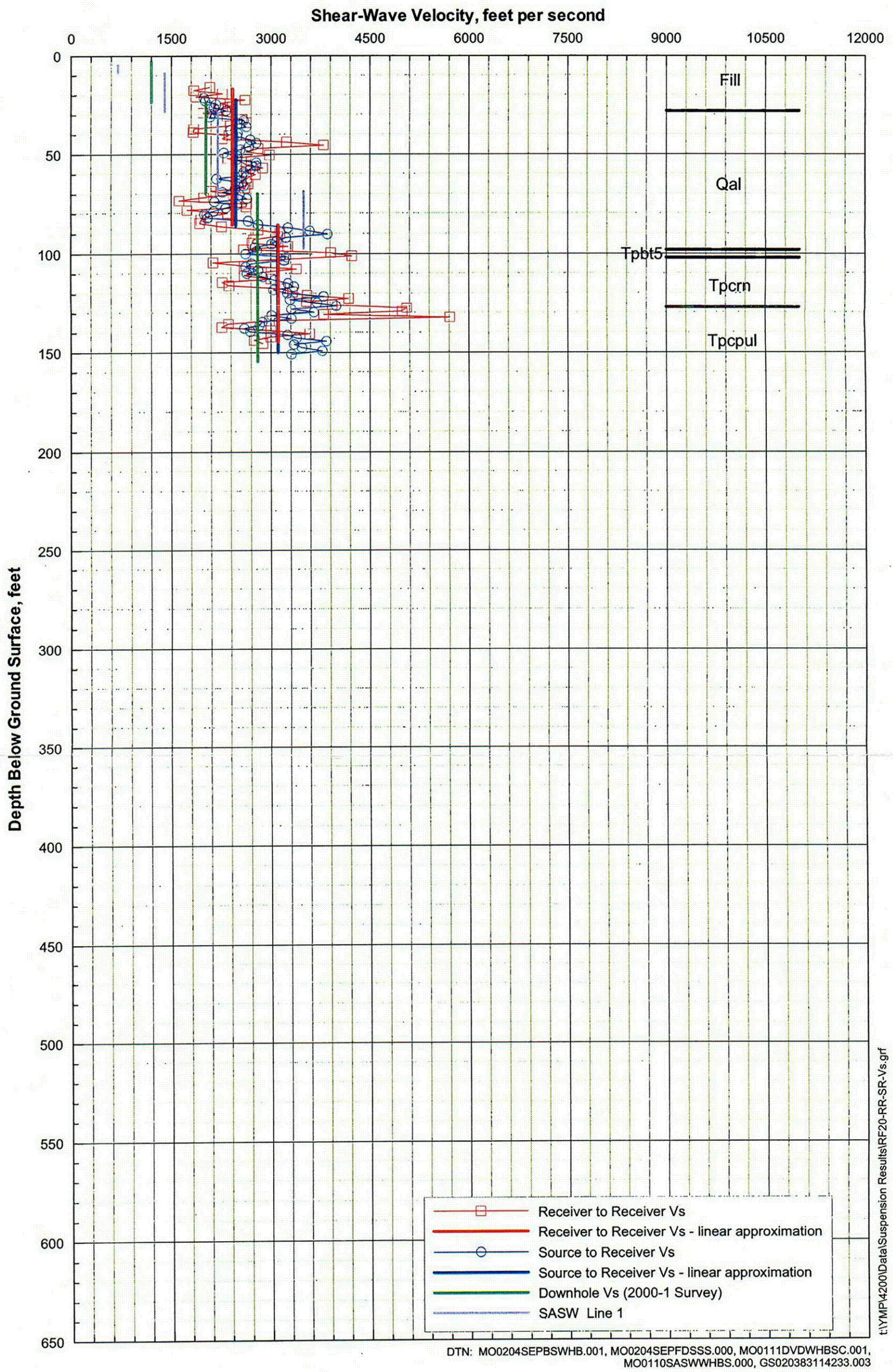

NOTE: Downhole and SASW velocities are shown for comparison.

Figure VII-8. Shear-Wave Velocity (v_S) from Suspension Seismic Source-to-Receiver and Receiver-to-Receiver Data at Borehole RF#20.

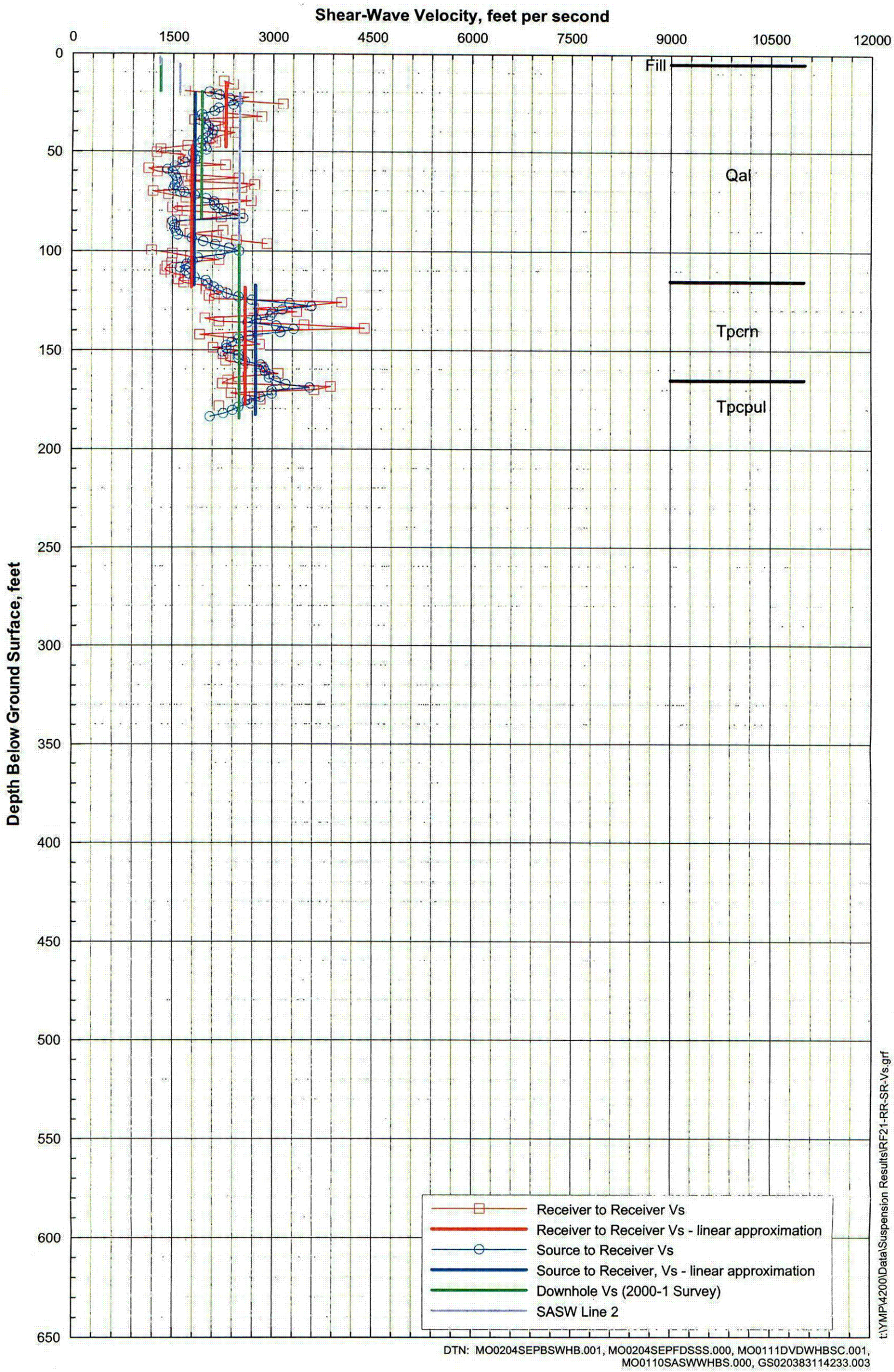

NOTE: Downhole and SASW velocities are shown for comparison.

Figure VII-9. Shear-Wave Velocity (v_S) from Suspension Seismic Source-to-Receiver and Receiver-to-Receiver Data at Borehole RF#21.

C13

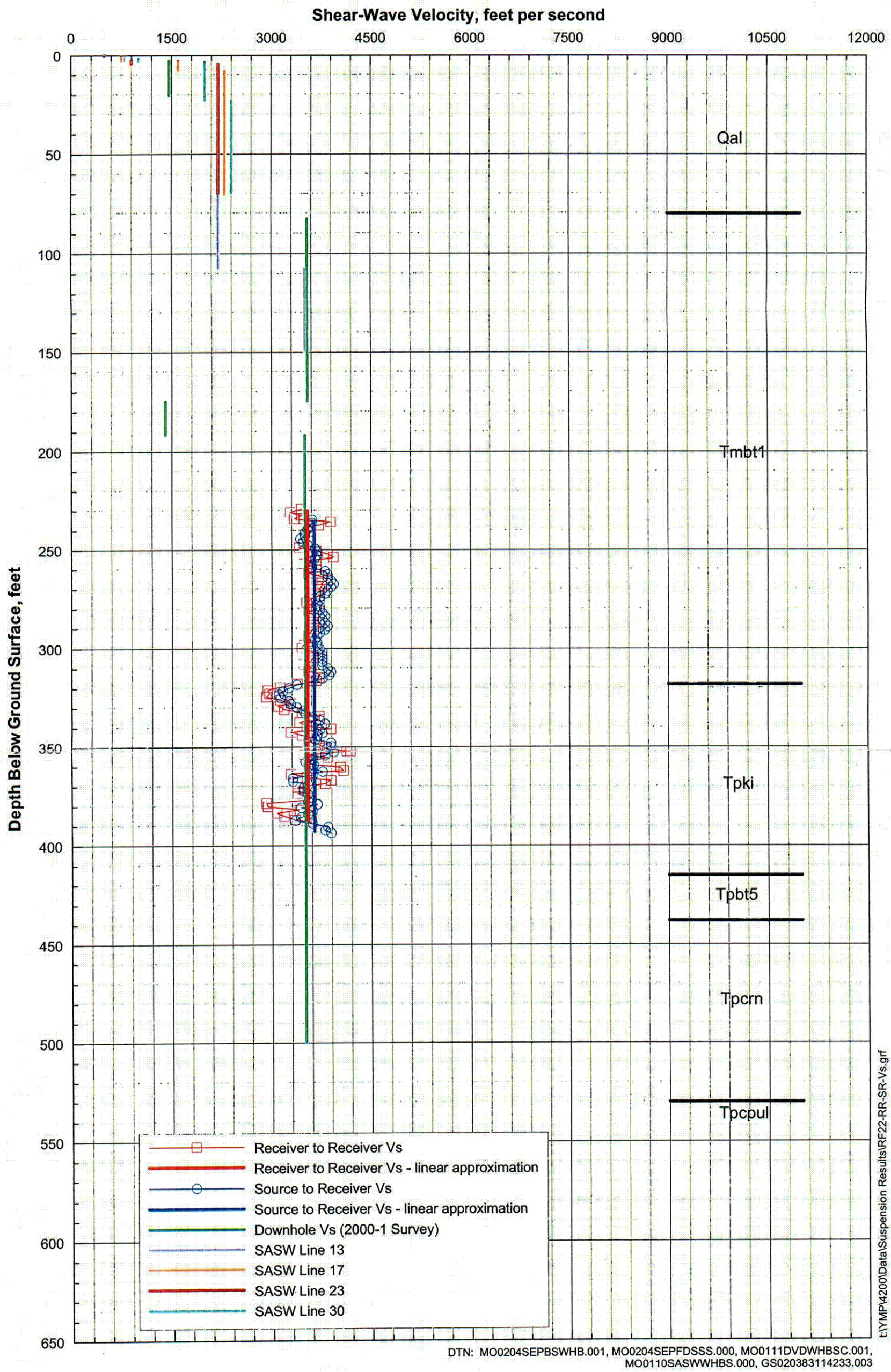

NOTE: Downhole and SASW velocities are shown for comparison.

Figure VII-10. Shear-Wave Velocity (v_S) from Suspension Seismic Source-to-Receiver and Receiver-to-Receiver Data at Borehole RF#22.

C14

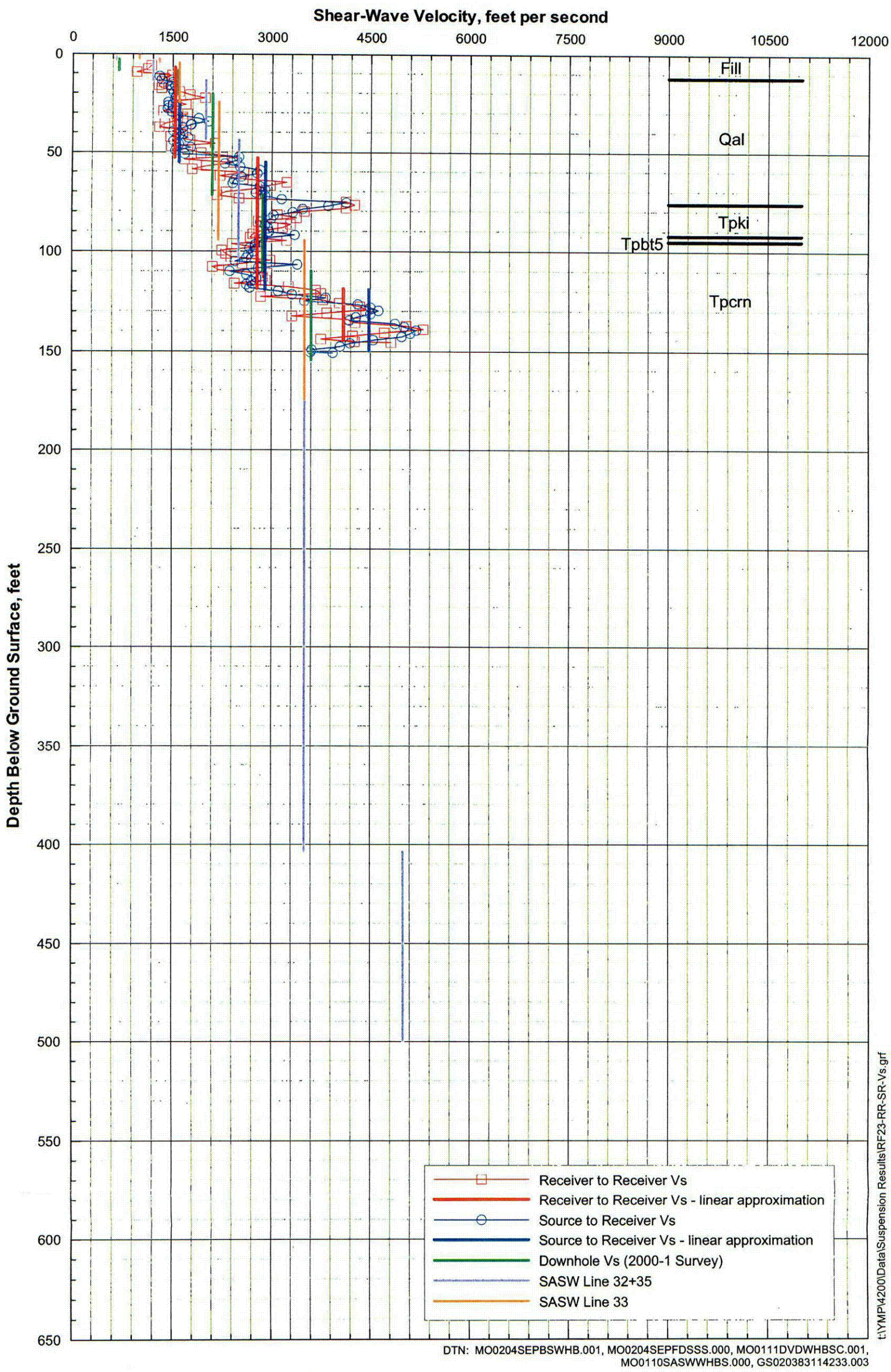

NOTE: Downhole and SASW velocities are shown for comparison.

Figure VII-11. Shear-Wave Velocity (v_S) from Suspension Seismic Source-to-Receiver and Receiver-to-Receiver Data at Borehole RF#23.

C15

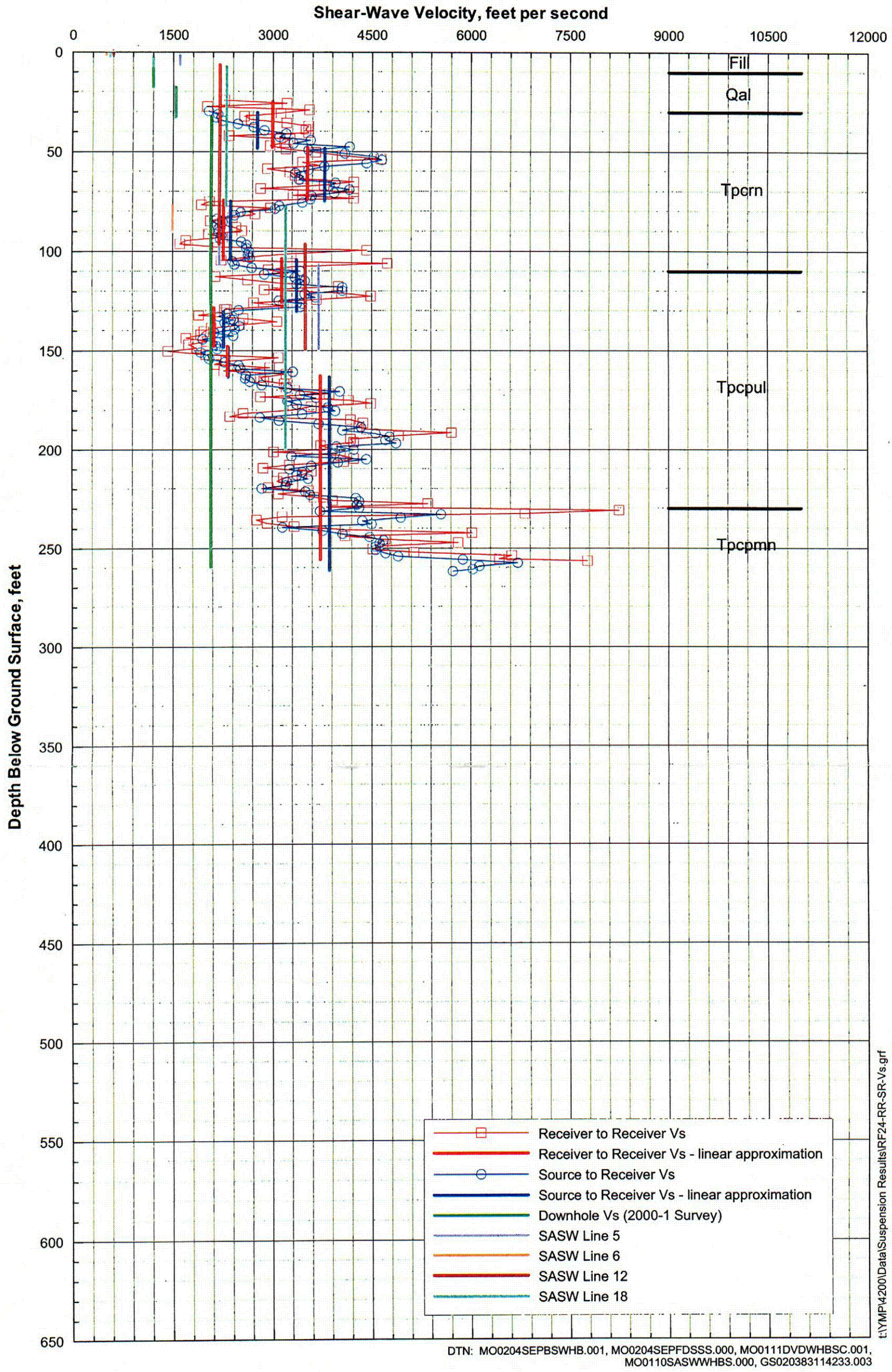

NOTE: Downhole and SASW velocities are shown for comparison.

Figure VII-12. Shear-Wave Velocity (v_S) from Suspension Seismic Source-to-Receiver and Receiver-to-Receiver Data at Borehole RF#24.

C16

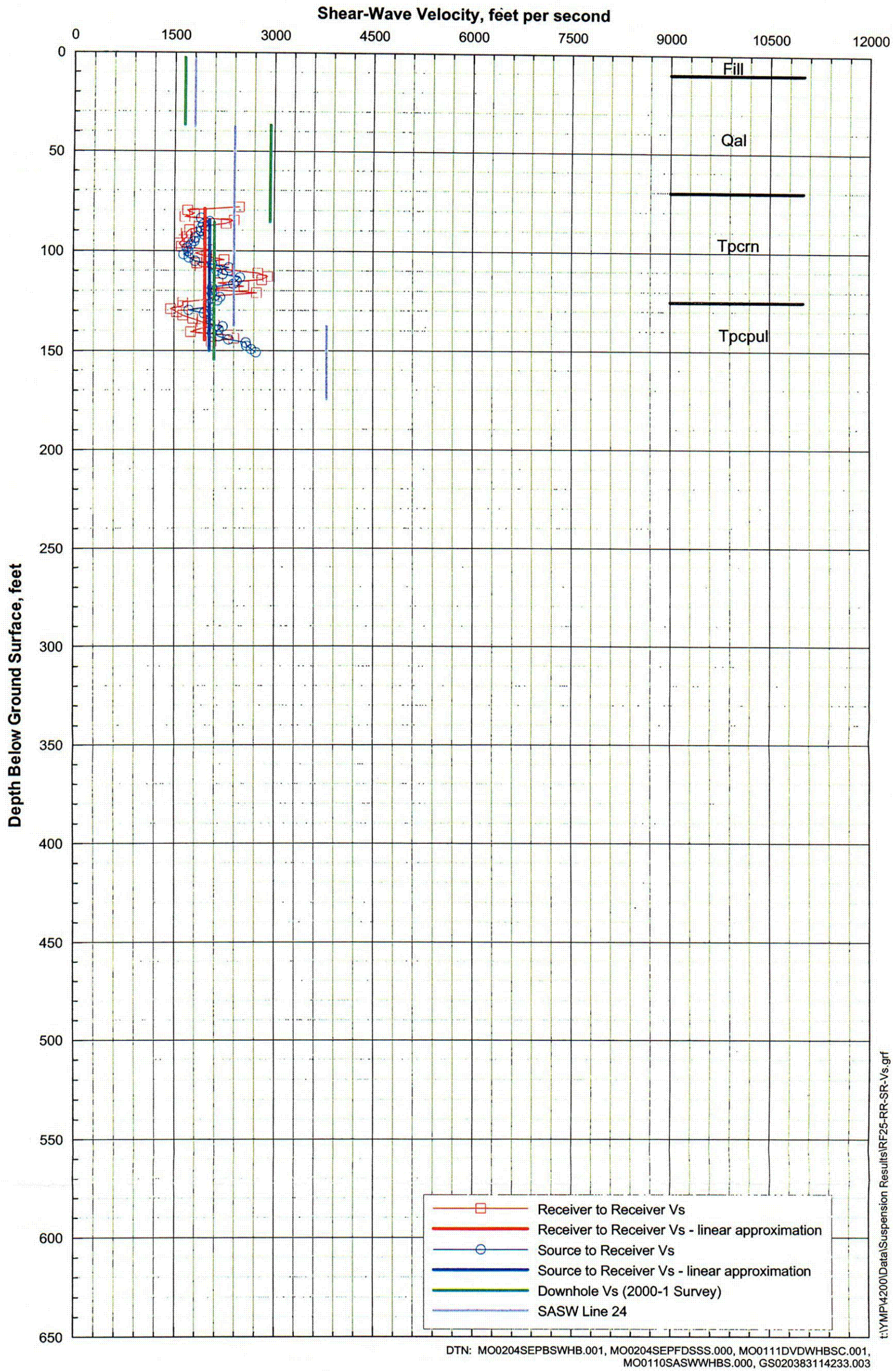

NOTE: Downhole and SASW velocities are shown for comparison.

Figure VII-13. Shear-Wave Velocity (v_S) from Suspension Seismic Source-to-Receiver and Receiver-to-Receiver Data at Borehole RF#25.

C17

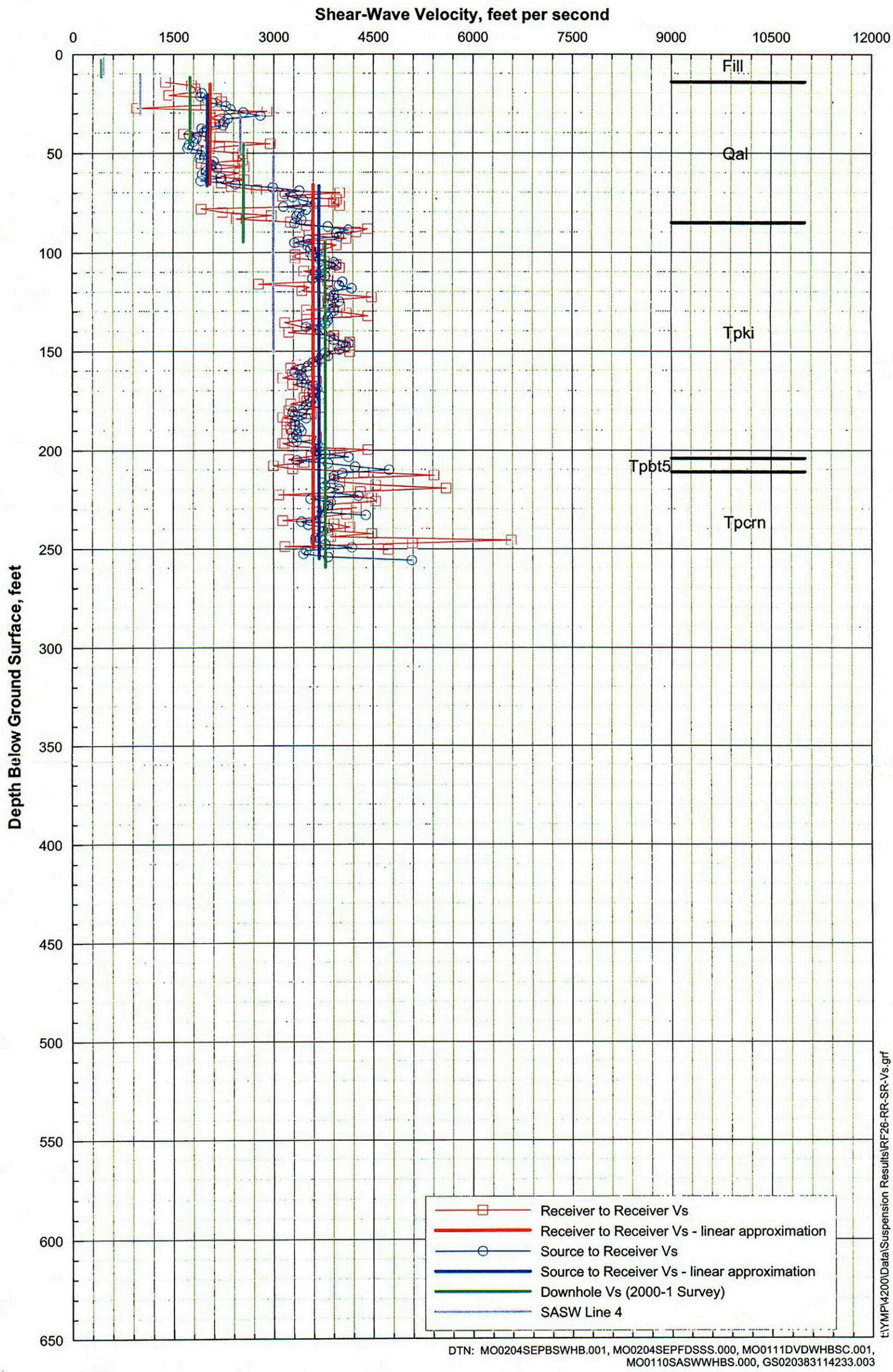

NOTE: Downhole and SASW velocities are shown for comparison.

Figure VII-14. Shear-Wave Velocity (v_S) from Suspension Seismic Source-to-Receiver and Receiver-to-Receiver Data at Borehole RF#26.

C18

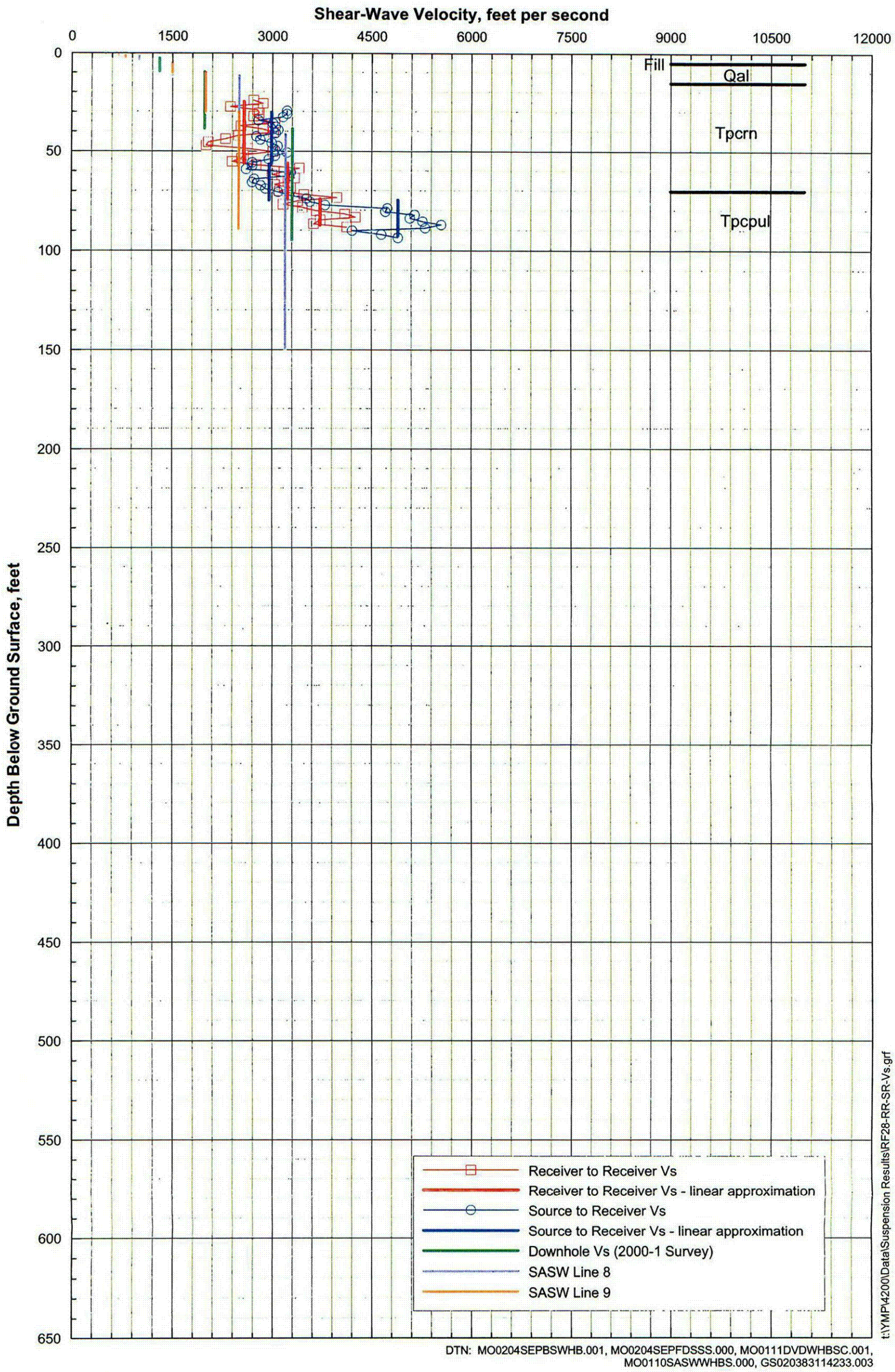

NOTE: Downhole and SASW velocities are shown for comparison.

Figure VII-15. Shear-Wave Velocity (v_S) from Suspension Seismic Source-to-Receiver and Receiver-to-Receiver Data at Borehole RF#28.

C19

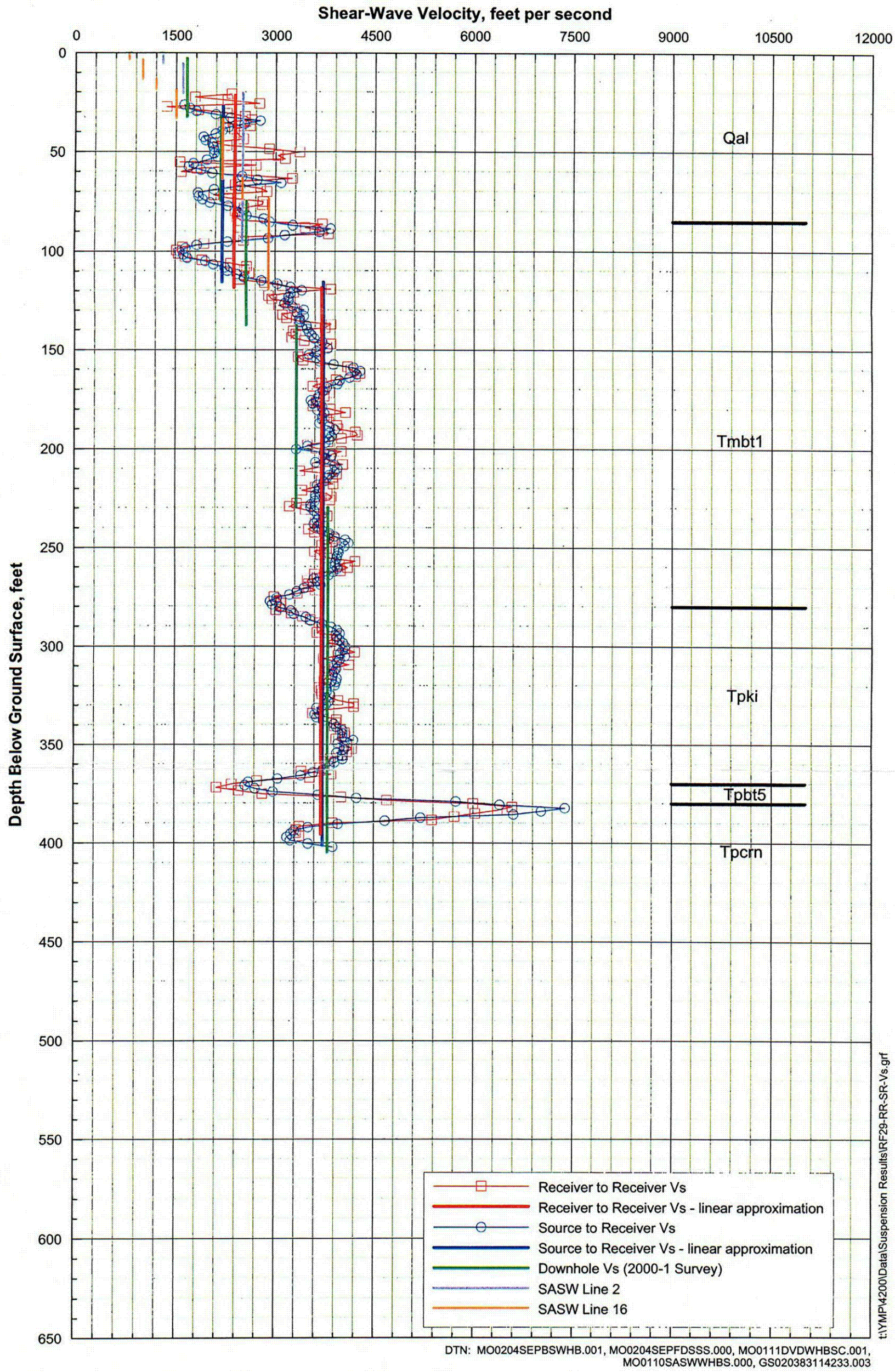

NOTE: Downhole and SASW velocities are shown for comparison.

Figure VII-16. Shear-Wave Velocity (v_S) from Suspension Seismic Source-to-Receiver and Receiver-to-Receiver Data at Borehole RF#29.

C20

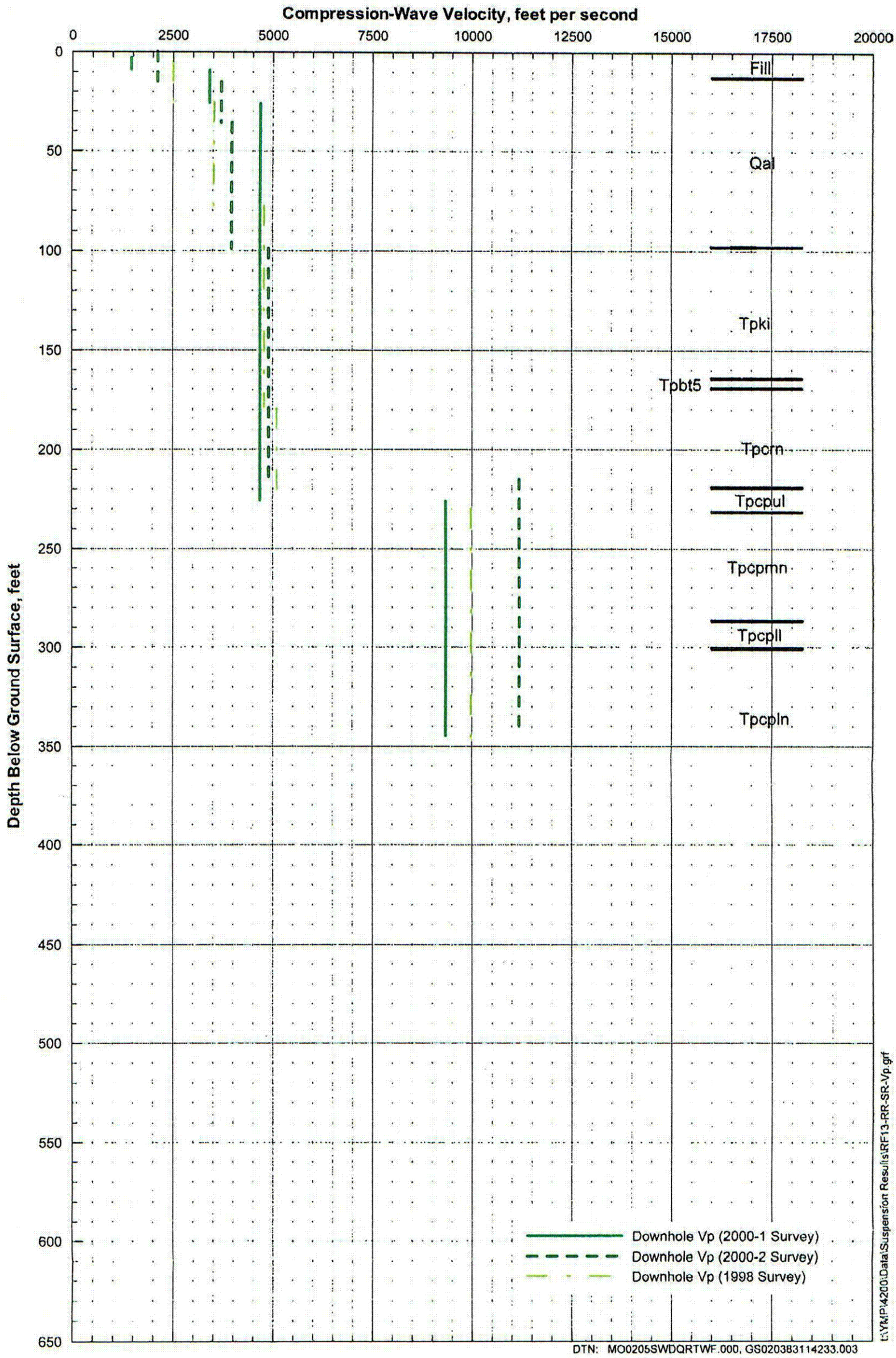

NOTE: Although no compression wave data were available from the suspension seismic survey, this plot is included to show the agreement between the three downhole velocity profiles.

Figure VII-17. Compression-Wave Velocity Profiles (v_p) from Downhole Seismic Surveys at Borehole RF#13.

C21

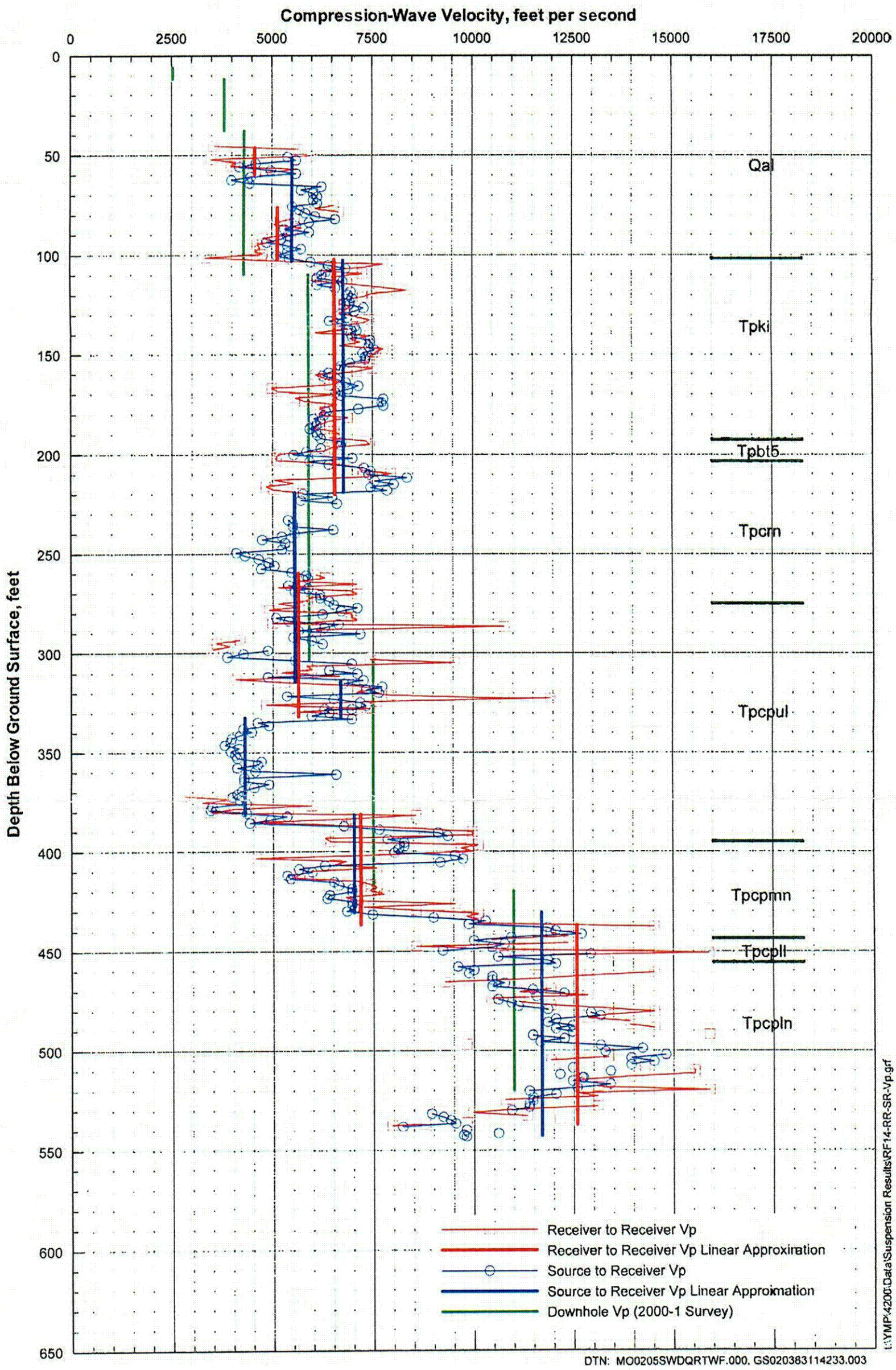

NOTE: Downhole velocities are shown for comparison.

Figure VII-18. Compression-Wave Velocity (v_p) from Suspension Seismic Source-to-Receiver and Receiver-to-Receiver Data at Borehole RF#14.

C22

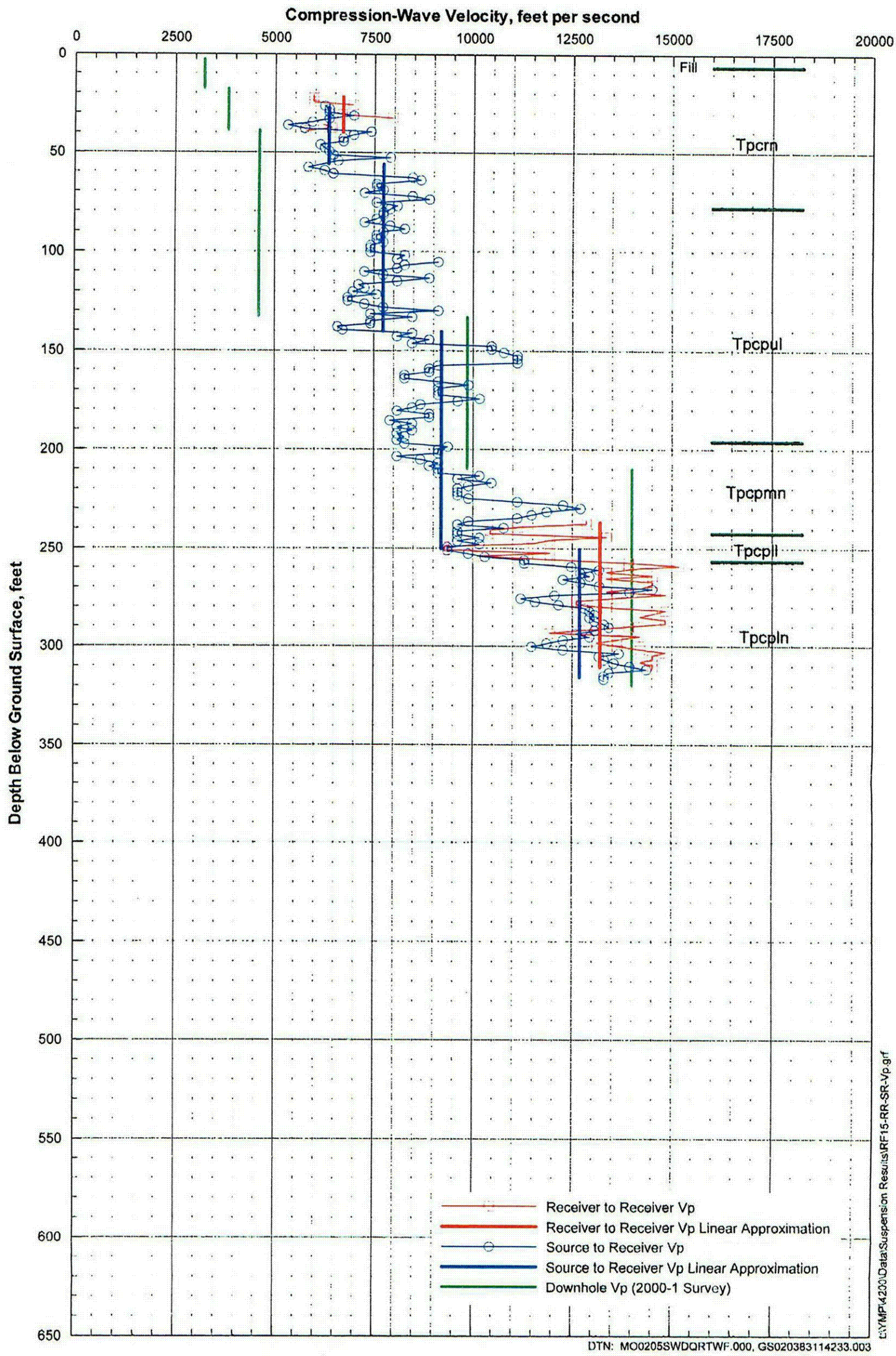

NOTE: Downhole velocities are shown for comparison.

Figure VII-19. Compression-Wave Velocity (v_p) from Suspension Seismic Source-to-Receiver and Receiver-to-Receiver Data at Borehole RF#15.

C23

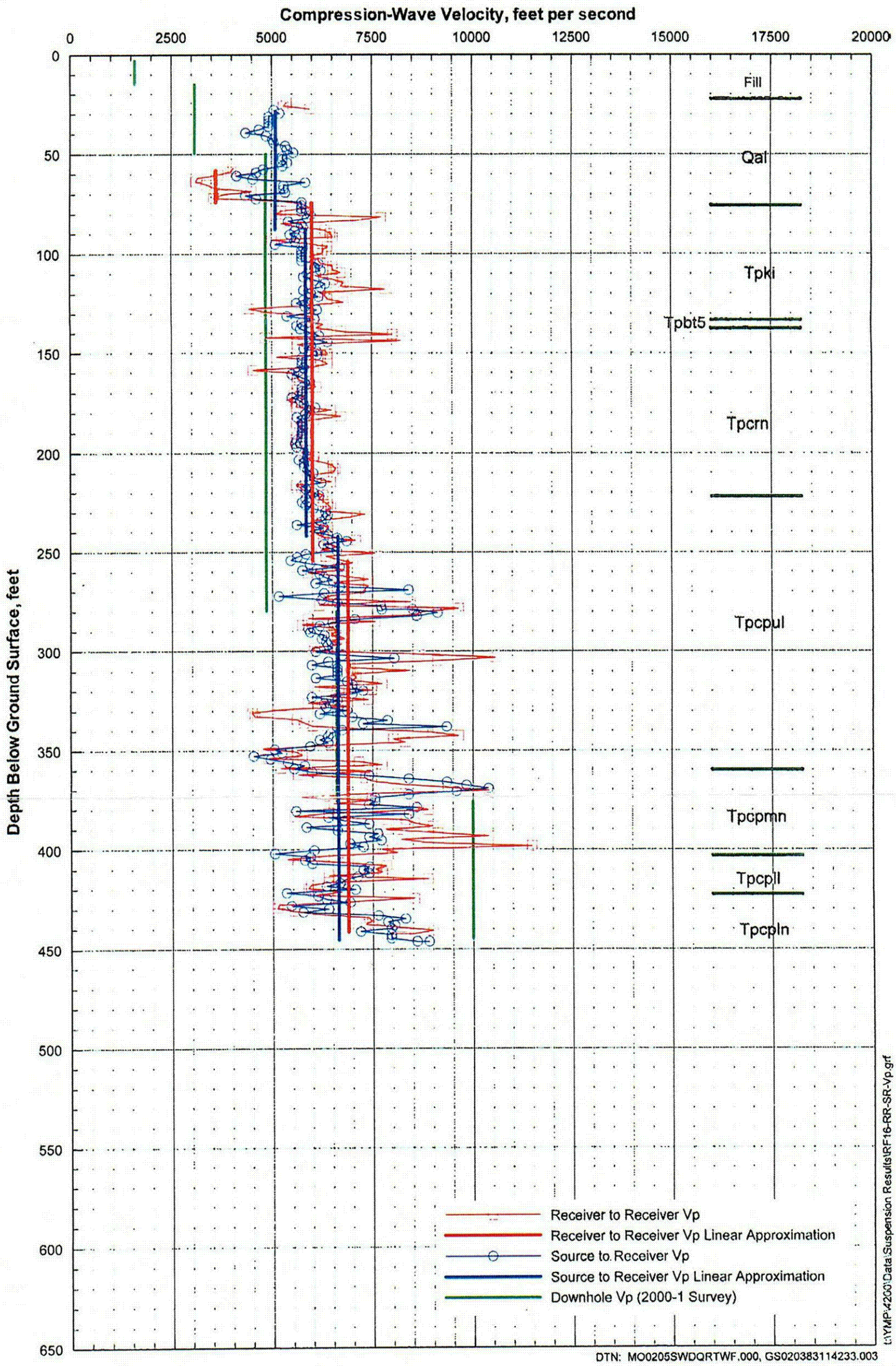

NOTE: Downhole velocities are shown for comparison.

Figure VII-20. Compression-Wave Velocity (v_p) from Suspension Seismic Source-to-Receiver and Receiver-to-Receiver Data at Borehole RF#16.

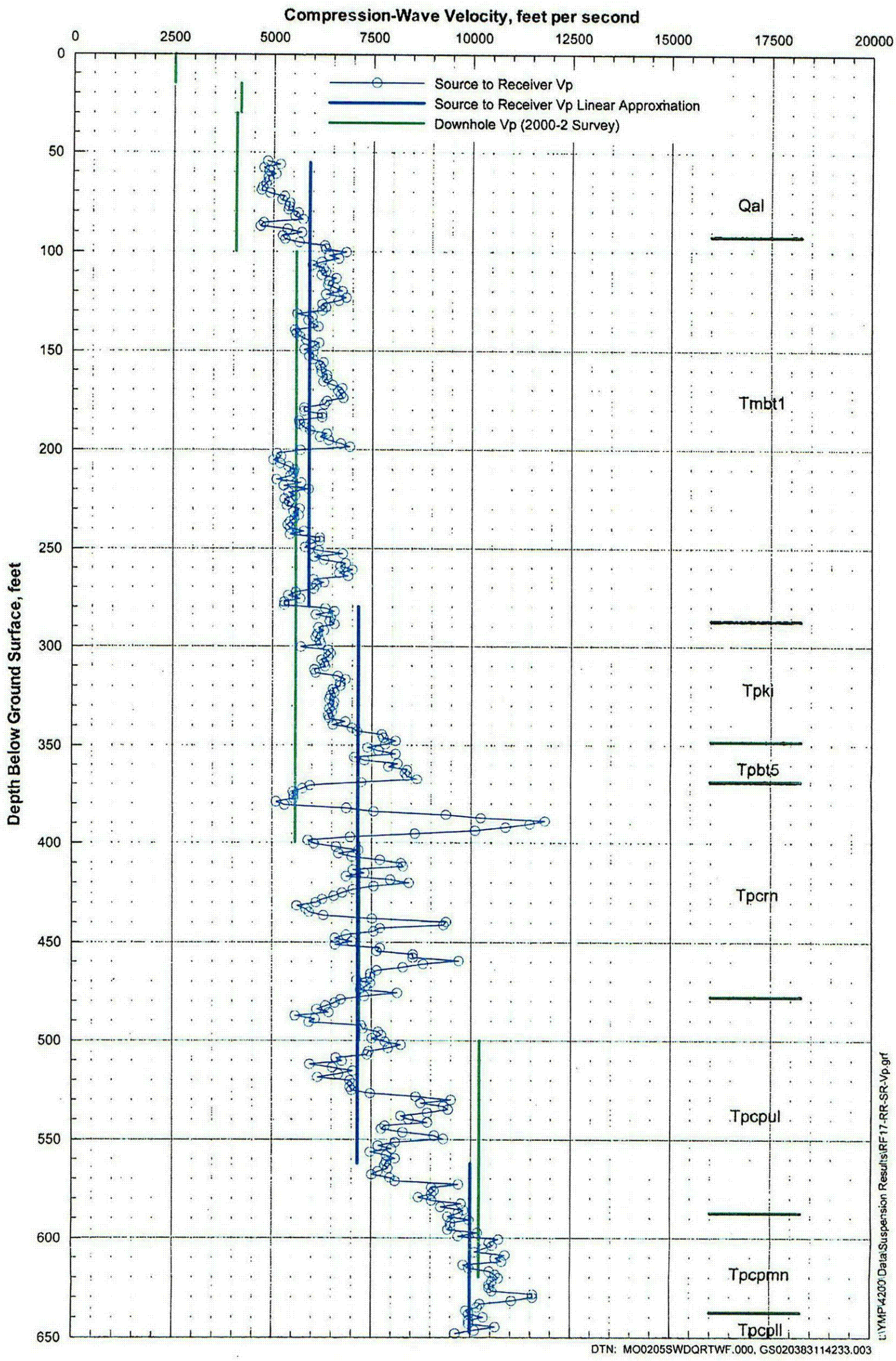

NOTE: Downhole velocities are shown for comparison.
No data for receiver-to-receiver.

Figure VII-21. Compression-Wave Velocity (v_p) from Suspension Seismic Source-to-Receiver Data at Borehole RF#17.

C25

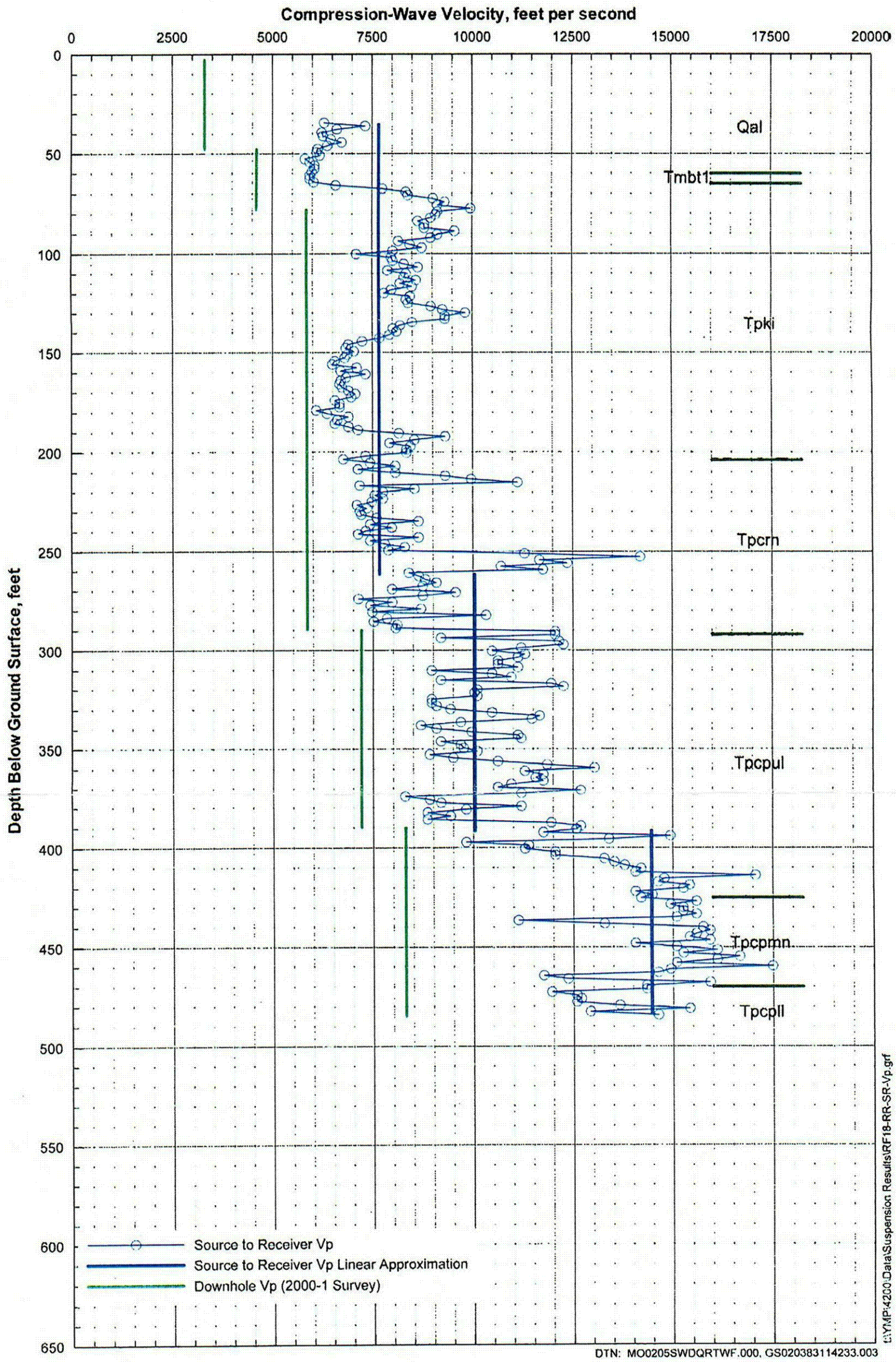

NOTE: Downhole velocities are shown for comparison.
No data for receiver-to-receiver.

Figure VII-22. Compression-Wave Velocity (v_p) from Suspension Seismic Source-to-Receiver Data at Borehole RF#18.

C20

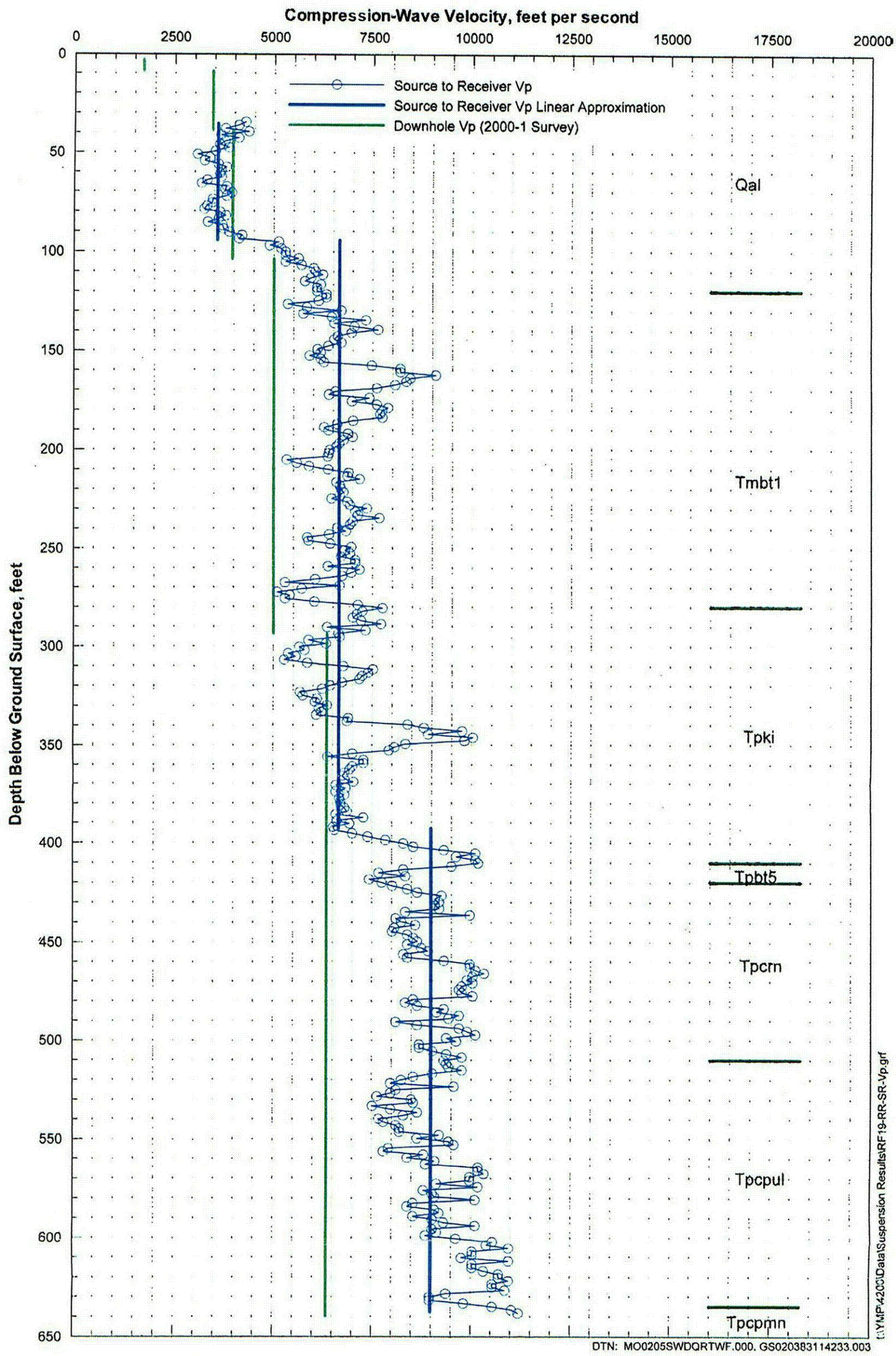

NOTE: Downhole velocities are shown for comparison.
No data for receiver-to-receiver.

Figure VII-23. Compression-Wave Velocity (v_p) from Suspension Seismic Source-to-Receiver Data at Borehole RF#19.

C27

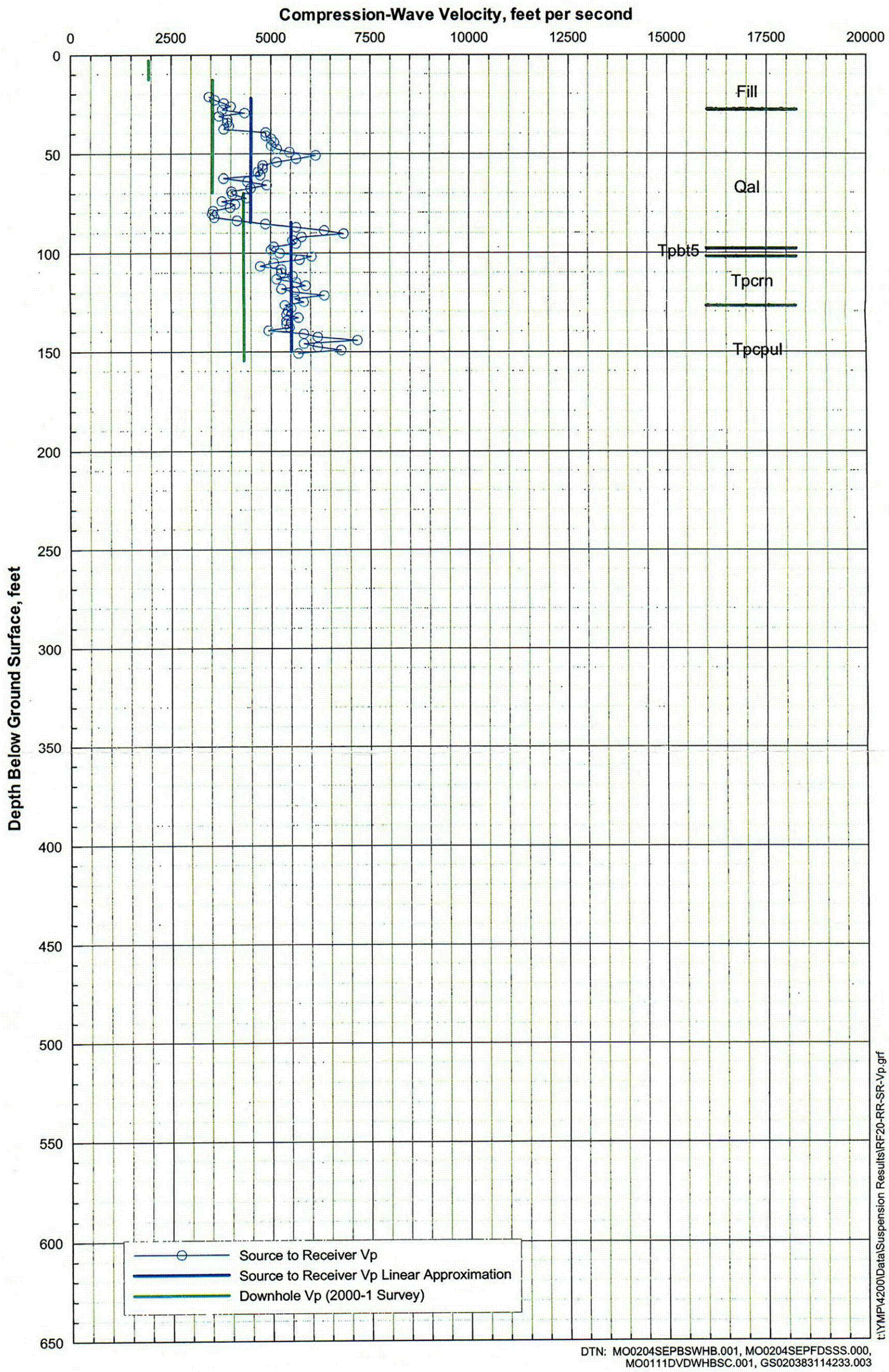

NOTE: Downhole velocities are shown for comparison.
No data for receiver-to-receiver.

Figure VII-24. Compression-Wave Velocity (v_p) from Suspension Seismic Source-to-Receiver Data at Borehole RF#20.

C28

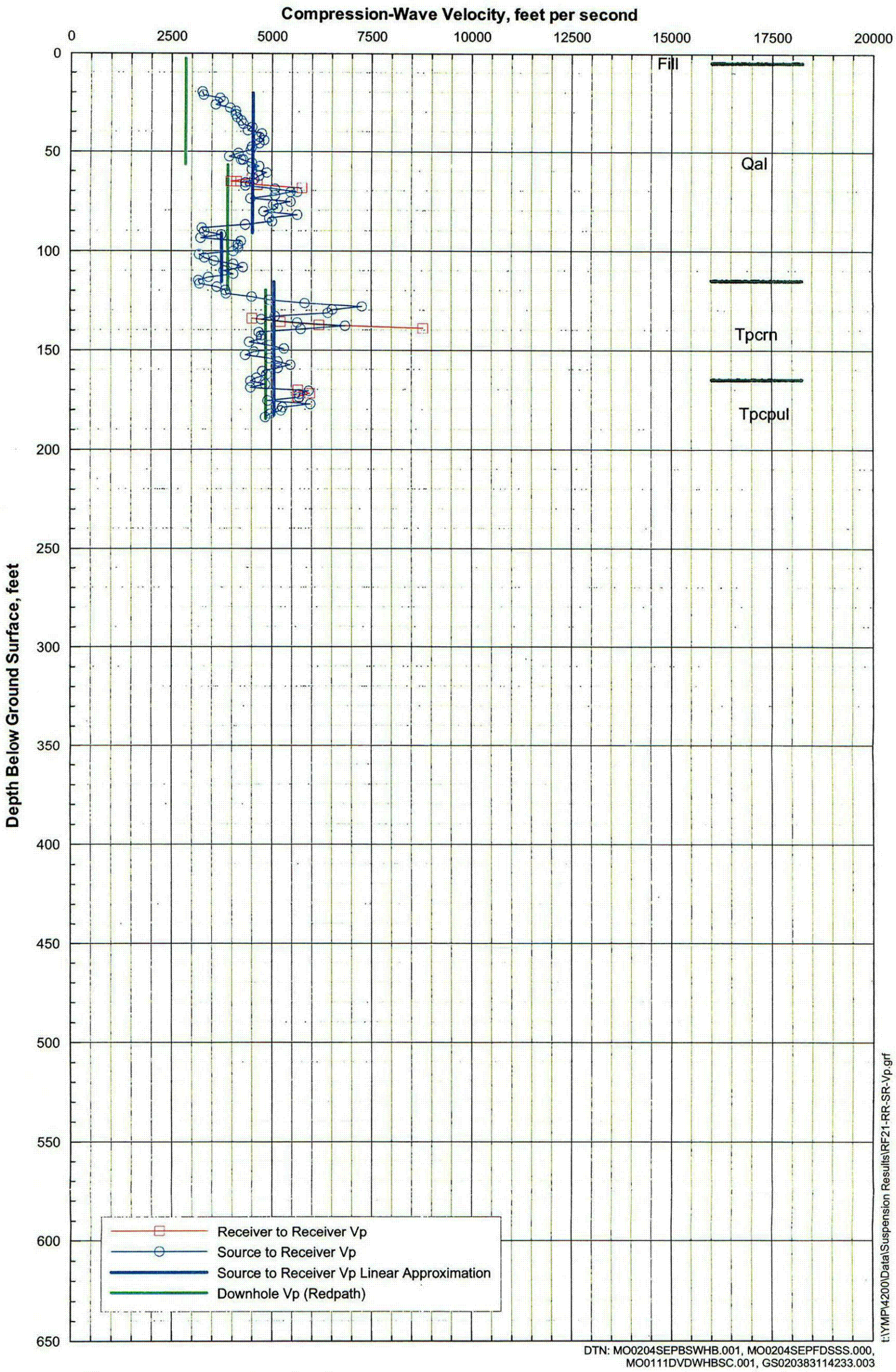

NOTE: Downhole velocities are shown for comparison.
Linear Approximation of receiver-to-receiver
not applicable due to insuficience of data points

Figure VII-25. Compression-Wave Velocity (v_p) from Suspension Seismic Source-to-Receiver and Receiver-to-Receiver Data at Borehole RF#21.

C29

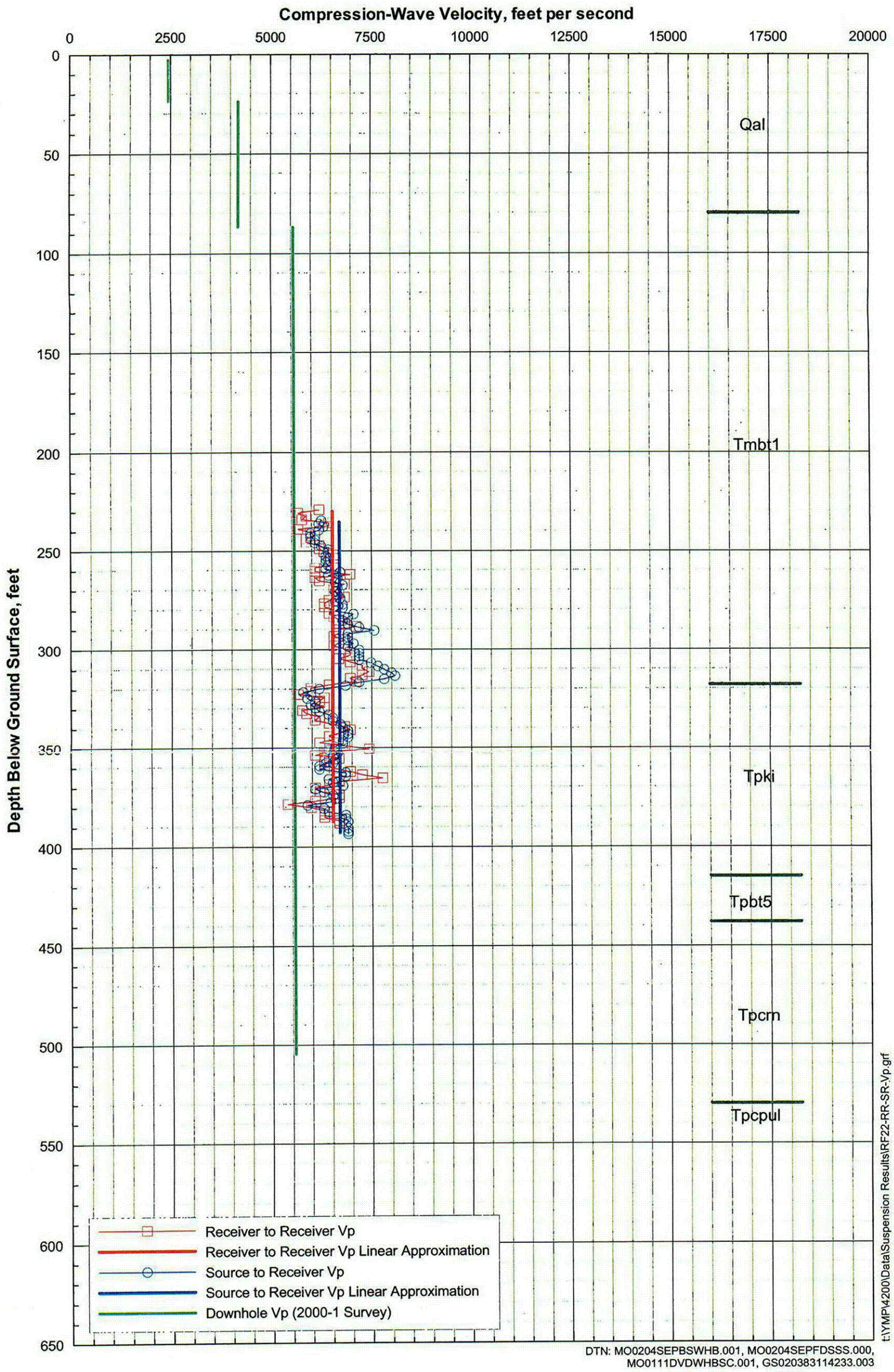

NOTE: Downhole velocities are shown for comparison.

Figure VII-26. Compression-Wave Velocity (v_p) from Suspension Seismic Source-to-Receiver and Receiver-to-Receiver Data at Borehole RF#22.

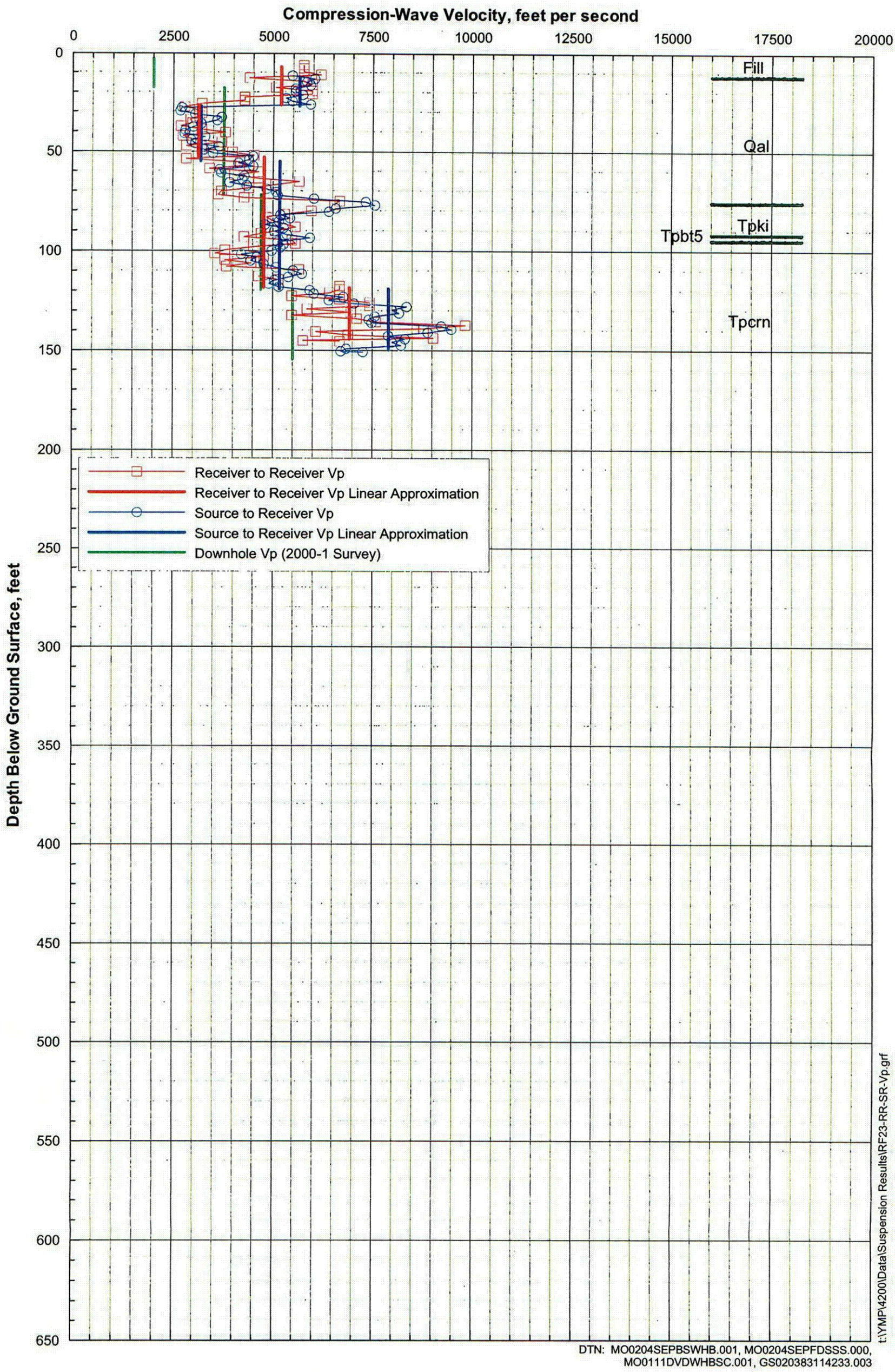

NOTE: Downhole velocities are shown for comparison.

Figure VII-27. Compression-Wave Velocity (v_p) from Suspension Seismic Source-to-Receiver and Receiver-to-Receiver Data at Borehole RF#23.

C31

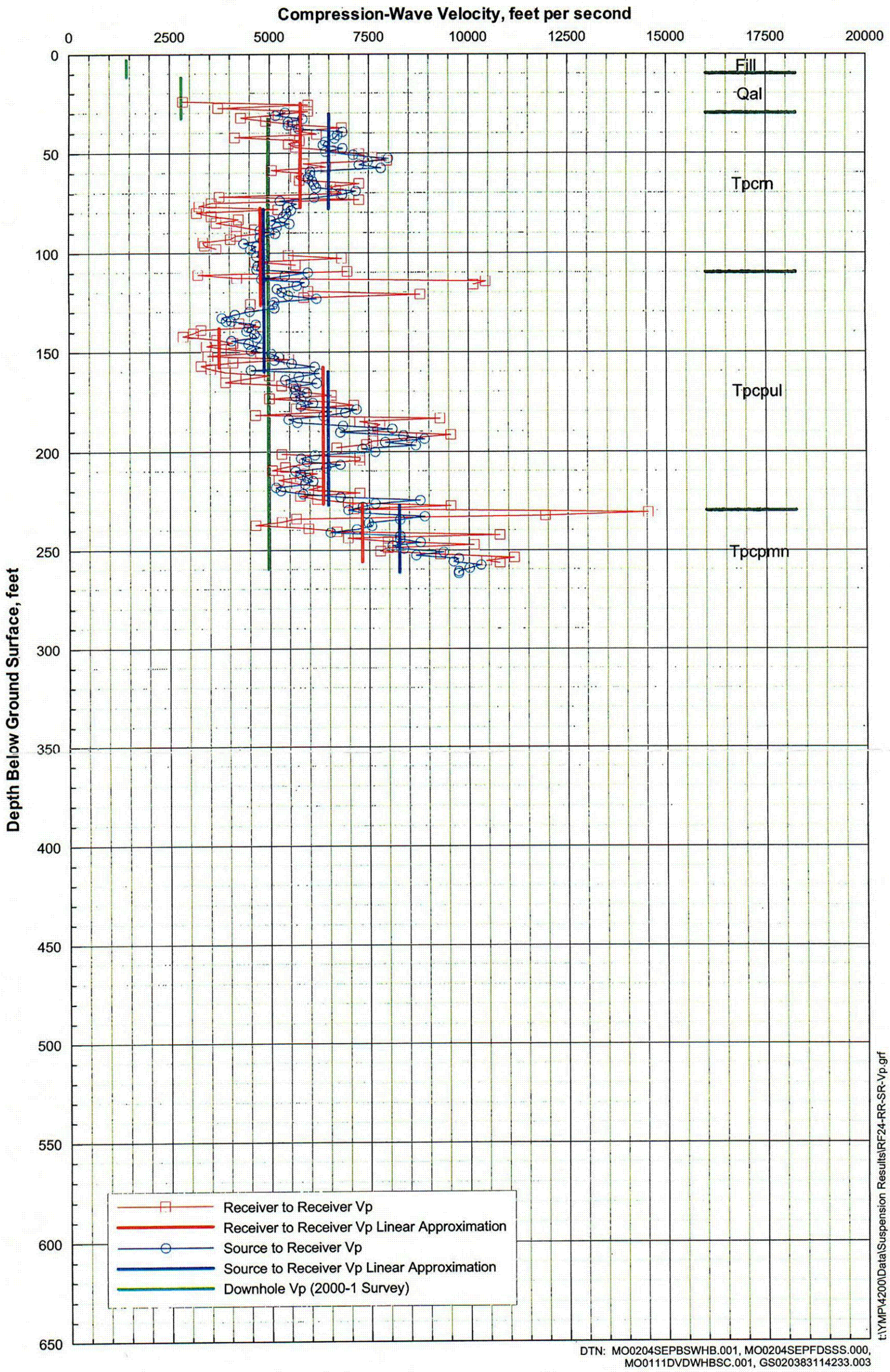

NOTE: Downhole velocities are shown for comparison.

Figure VII-28. Compression-Wave Velocity (v_p) from Suspension Seismic Source-to-Receiver and Receiver-to-Receiver Data at Borehole RF#24.

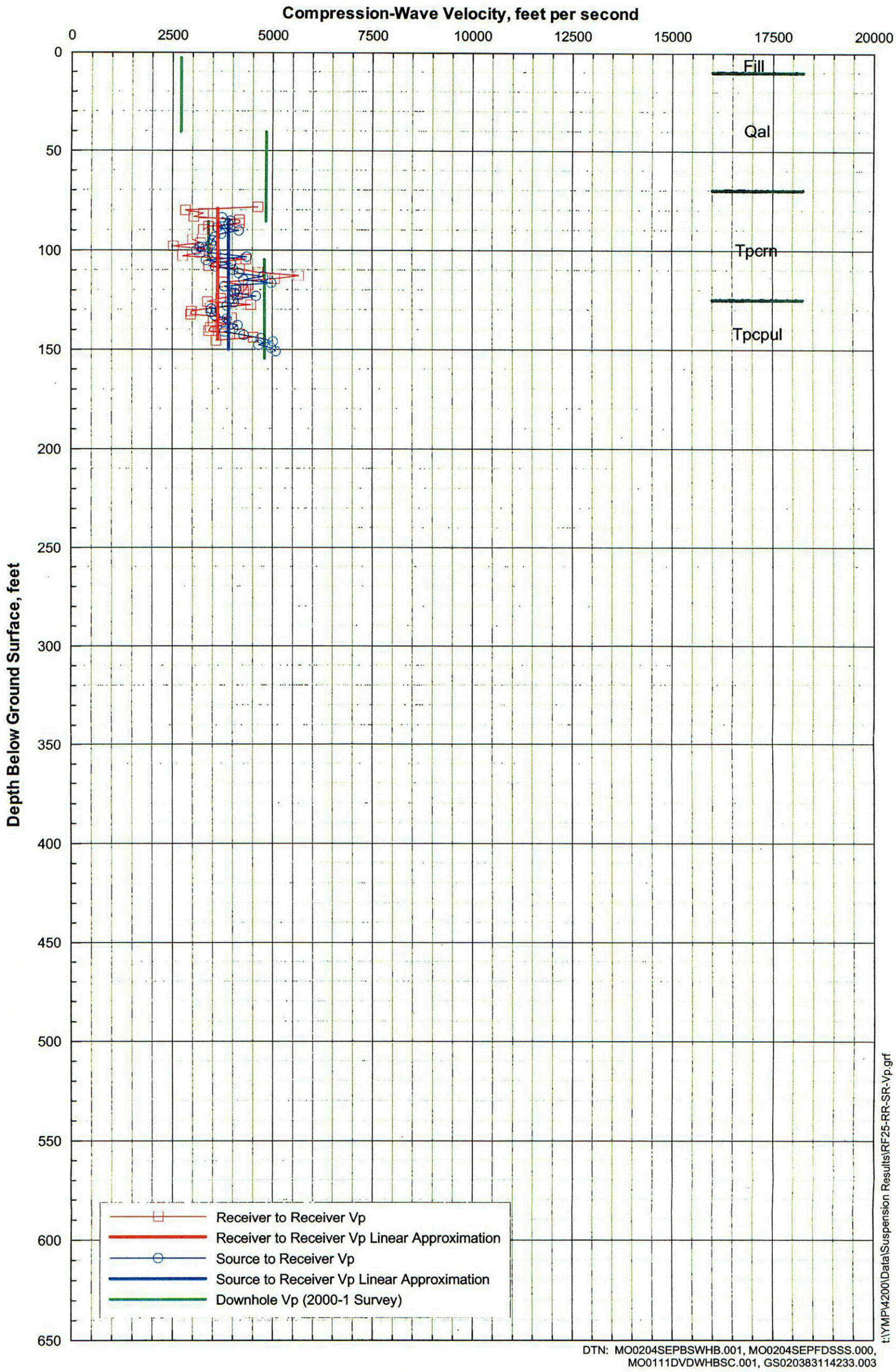

NOTE: Downhole velocities are shown for comparison.

Figure VII-29. Compression-Wave Velocity (v_p) from Suspension Seismic Source-to-Receiver and Receiver-to-Receiver Data at Borehole RF#25.

C33

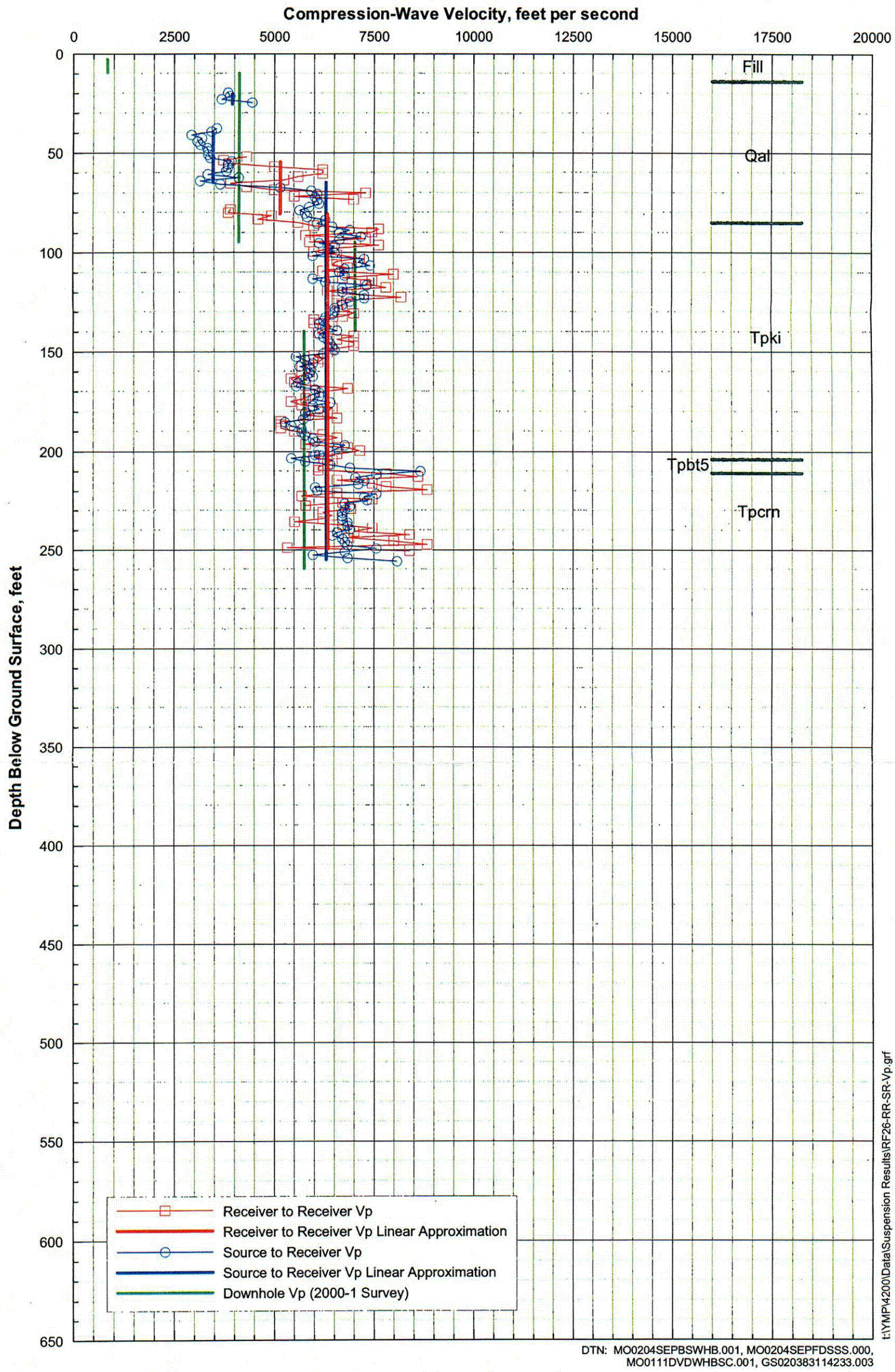

NOTE: Downhole velocities are shown for comparison.

Figure VII-30. Compression-Wave Velocity (v_p) from Suspension Seismic Source-to-Receiver and Receiver-to-Receiver Data at Borehole RF#26.

C34

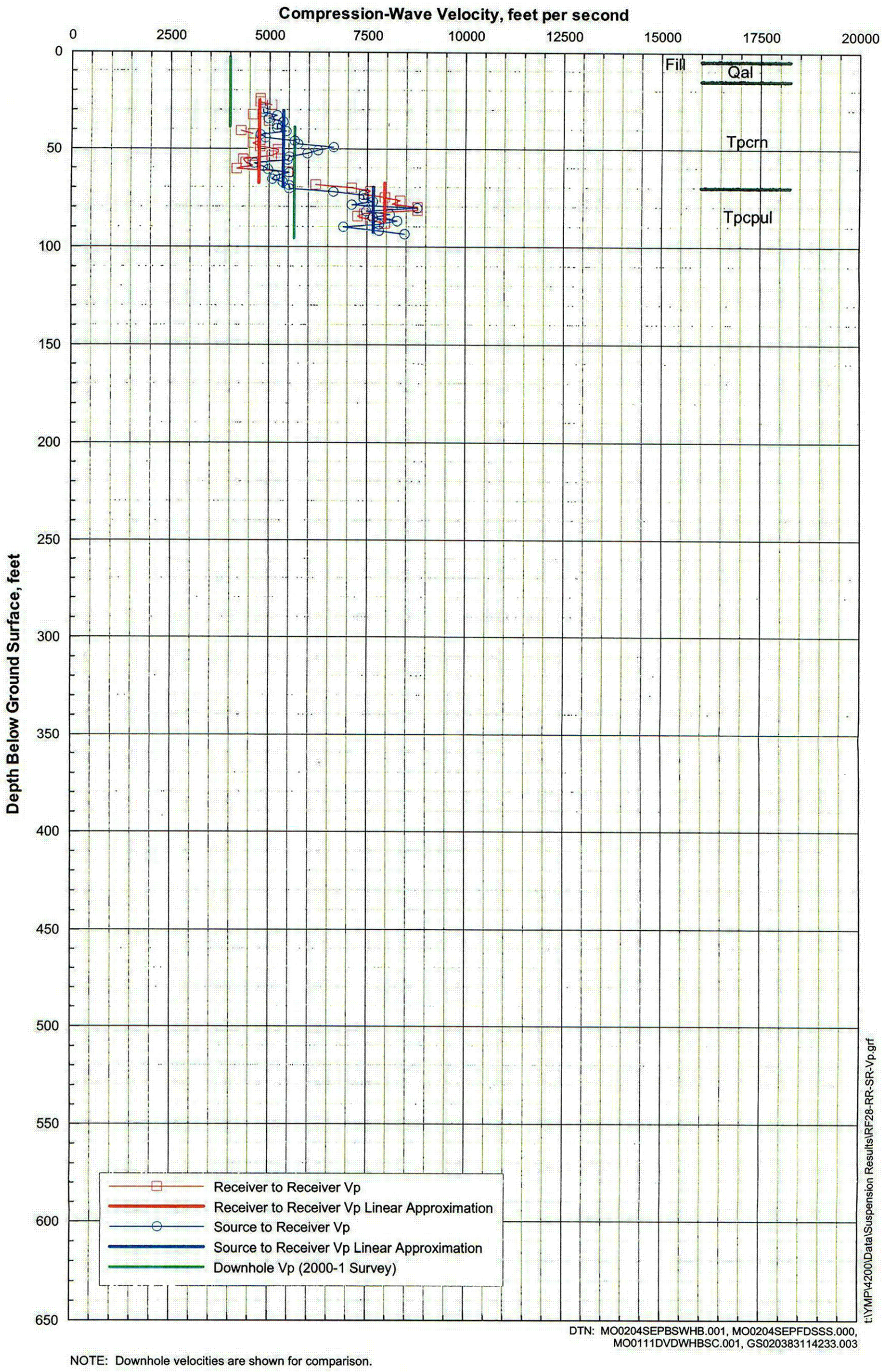

DTN: MO0204SEPBSWHB.001, MO0204SEPFDSSS.000, MO0111DVDWHBSC.001, GS020383114233.003

NOTE: Downhole velocities are shown for comparison.

Figure VII-31. Compression-Wave Velocity (v_p) from Suspension Seismic Source-to-Receiver and Receiver-to-Receiver Data at Borehole UE-RF#28.

C35

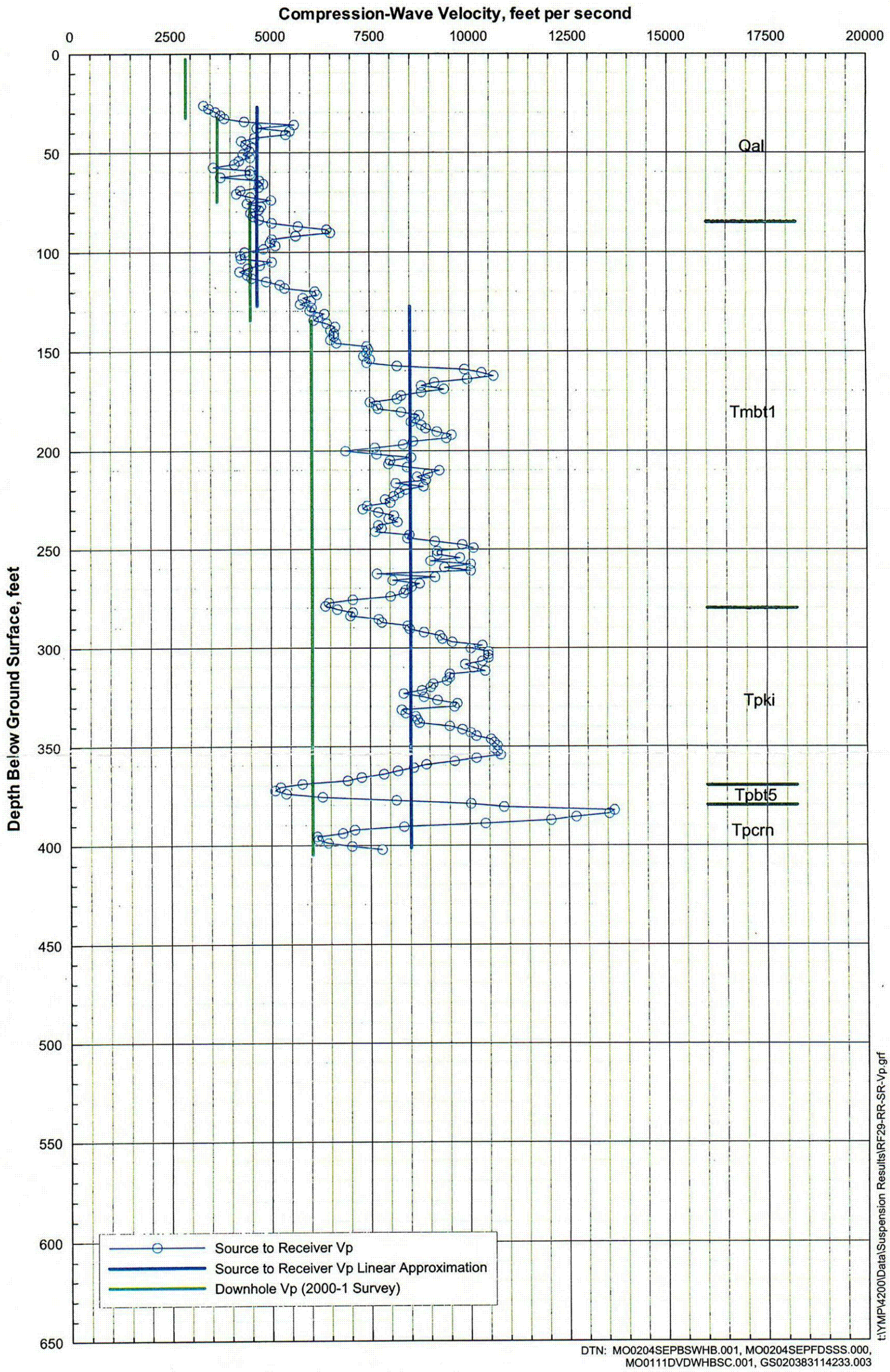

NOTE: Downhole velocities are shown for comparison.
No data for receiver-to-receiver.

Figure VII-32. Compression-Wave Velocity (v_p) from Suspension Seismic Source-to-Receiver Data at Borehole RF#29.

C36